Review

Israel Journal of Chemistry

DOI: 10.1002/ijch.200((full DOI will be filled in by the editorial staff))

Recent Advances in Electrochemical, Ni-Catalyzed C–C Bond Formation

Mareena C. Franke[a] and Daniel J. Weix*[a]

Abstract: Nickel-catalyzed cross-electrophile coupling (XEC) is an efficient method to form carbon–carbon bonds and has become an important tool for building complex molecules. While XEC has most often used stoichiometric metal reductants, these transformations can also be driven electrochemically. Electrochemical XEC (eXEC) is attractive because it can increase the greenness of XEC and this potential has resulted in numerous advances in recent years. The focus of this review is on electrochemical, Ni-catalyzed carbon–carbon bond forming reactions reported since 2010 and is categorized by the type of anodic half reaction: sacrificial anode, sacrificial reductant, and convergent paired electrolysis. The key developments are highlighted and the need for more scalable options is discussed.

Keywords: nickel catalysis • electrochemistry • sacrificial anode • sacrificial reductant • paired electrolysis

1. Introduction

The use of electrochemistry to drive nickel chemistry has been known for several decades. In the early 1970s, it was shown that $Ni(acac)_2$ (nickel(II) acetylacetonate) could be electrochemically reduced to $Ni(cod)_2$ (bis(cyclooctadiene)nickel(0)).[1] The first example of using electrochemically-generated nickel complexes catalytically was in 1976, when Jennings et al. reported reductive homocoupling of alkyl, benzylic, and aryl halides using a sacrificial anode in an undivided cell.[2] Since these initial reports, there have been many developments in electrochemical metal-catalysis which cannot be fully captured here, but a number of reviews on this topic have been published[3–5] including a comprehensive review by Jutand in 2008.[6] In addition, books with practical information on setting up organic electrochemical reactions are available.[7,8] Reviews on more recent reports of electrochemical transformations that extend beyond the scope of this review have also been written. Rueping and co-workers compared traditional, photochemical, and electrochemical methods to form C–C bonds.[9] Mathew and co-workers reviewed Ni-catalyzed electrochemical C–C and C–heteroatom bond formations.[10] Ackermann and co-workers reviewed electrochemical, Ni-catalyzed C–H activation reactions that are reductive, redox-neutral, and oxidative.[11] Recent advances in Ni-catalyzed cross-coupling via paired electrolysis was reviewed by Li and co-workers.[12] A pair of reviews focusing on a variety of different transition metal-catalyzed electrochemical reactions were written by Swaroop, Rangappa, and co-workers and by De Sarkar and co-workers.[13,14] This manuscript focuses on the advancements in Ni-catalyzed cross-electrophile coupling to form C−C bonds via electrochemistry since 2010 until May 2023 and is organized by separating distinct anodic reaction into sections with further subsections for the type of bond formed (Figure 1).

Two important electrochemical metrics are current density (current applied / area of the working electrode) and Faradaic efficiency (moles of product / charge passed). Current density is important because current passed correlates with conversion; at a given Faradaic efficiency, a reaction that supports a higher current density will proceed faster. Unfortunately, there is not an agreed upon convention to report synthetic electrochemical reactions, so crucial details are often not available. For example, if the cathode area is missing the current density cannot be calculated. Indeed, current density can be challenging to compare because of different conventions used in calculating electrode surface area. For example, reticulated vitreous carbon (RVC) is typically described as 3-dimensional whereas nickel foam is 2-dimensional (only occasionally the thickness is given), so it is difficult to compare mA/cm^3 with mA/cm^2. Outside of electrode descriptions, reports of constant potential reactions often do not include the charge passed, so faradaic efficiency cannot be calculated. Even for constant current reactions where charge passed can easily be determined by the length of electrolysis, sometimes it is only stated that the reaction went until full conversion and the time is not given, again preventing calculation of Faradaic efficiency.

In addition to current density and Faradaic efficiency, the anodic half-reaction plays a role in determining the scalability of transition metal catalyzed electrochemical reactions. Most commonly, sacrificial anodes are used due to their simple setup and broad compatibility. The anode forms stoichiometric metal salts in solution as the reaction progresses to balance the charge needed for the cathodic reaction (Figure 1A). While metal salts formed are generally ignored, depending on the reaction and metal used, they can be beneficial or detrimental to the catalytic reaction. Additionally, the formation of metal

[a] Mareena C. Franke, Daniel J. Weix
Department of Chemistry, University of Wisconsin–Madison
Madison, Wisconsin 53706, United States
e-mail: dweix@wisc.edu

salts increases the solution conductivity, lowering the necessary cell potential. However, this method can be problematic for scale-up since the metal surface is corroded over time and the metal salt formed can be difficult to remove.

The use of a sacrificial reductant, such as an alkyl amine, provides an alternative anodic half-reaction (Figure 1B). While the reductant itself does not have enough driving force to reduce the catalyst, when a potential is applied, it can act as a source of electrons. In some cases, this method requires a divided cell to prevent the oxidation product of the sacrificial reductant from interfering with cathodic catalysis or "short-circuiting" the system by competing for reduction at the cathode. The catholyte and anolyte are therefore separated by a diaphragm, which can be a porous material or an ion-exchange membrane. This adds complexity for scale up, but also offers opportunities for using otherwise incompatible anodic chemistry to drive the reductive chemistry.

Convergent paired electrolysis involves two productive half reactions that together form a complete reaction. As an example, a substrate could be oxidized at the anode before entering the nickel catalytic cycle to form the desired product (Figure 1C). The redox reactivity of each substrate must be carefully matched to get a productive reaction. This method is undivided by necessity; however, reactions that utilize this method tend to have lower Faradaic efficiency due to the formation of short circuits (e.g., **I** being reduced at cathode instead of reacting with nickel in Figure 1).

We review the reported electrochemical Ni-catalyzed C–C bond forming reactions from 2010 onward below with the important characteristics of each work summarized. The emphasis of this review was on the electrochemical parts of the reaction rather than details of the substrate scope with the goal of providing an entry to the beginning organic electrochemist.

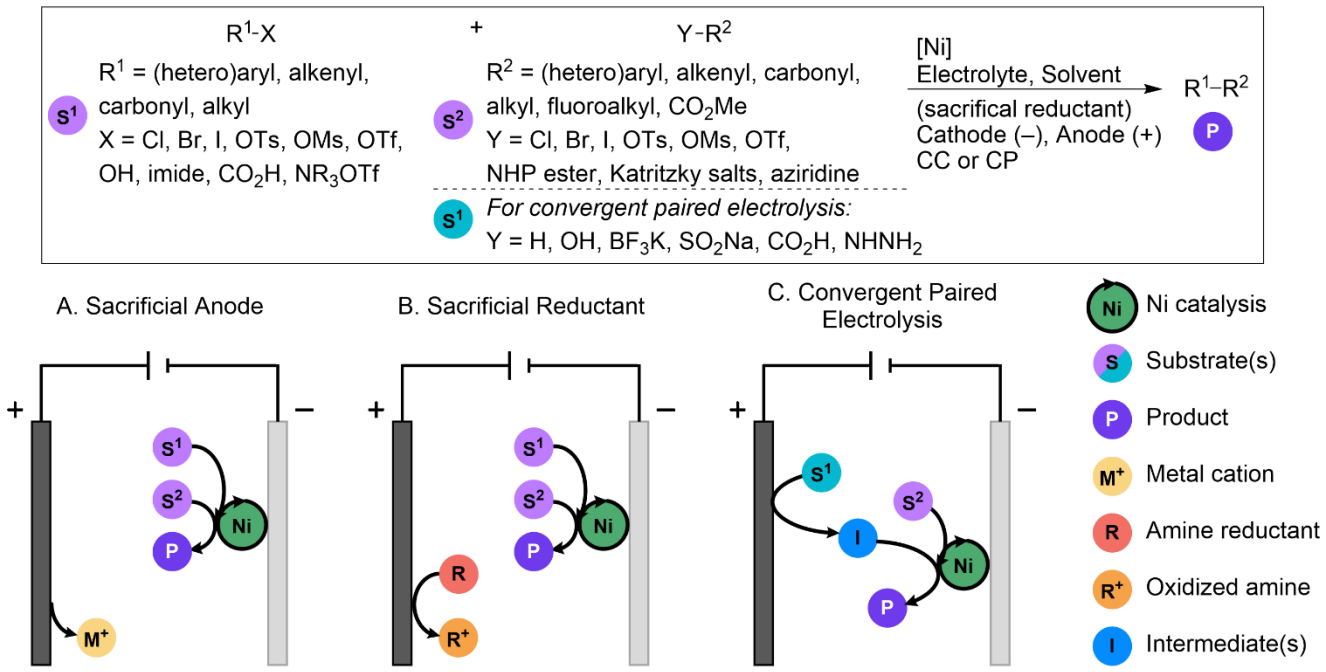

Figure 1. Schematic of different electrochemical strategies explored in this review. CC = Constant Current, CP = Constant Potential.

Mareena Franke received her B.A. in Chemistry and Physics at Coe College in Cedar Rapids, IA in 2019. Currently, she is a graduate student in the Weix lab at the University of Wisconsin–Madison. The focus of Mareena's research is on the development of greener, more scalable approaches to nickel-catalyzed cross-electrophile coupling, sustainable organic electrochemistry, and the use of electrochemistry to study nickel-catalyzed reactions.

Daniel Weix received his B.A. in Chemistry from Columbia University in 2000 (with Tom Katz) and obtained his PhD in 2005 from UC-Berkeley (with Jon Ellman). After postdoctoral training at Yale and Illinois (with John Hartwig), his independent career started at the University of Rochester in 2008. In 2017, Daniel moved to UW-Madison where he is currently the Wayland E. Noland Distinguished Professor of Chemistry. Daniel's research program is focused on developing new concepts in catalysis, the study of reaction mechanisms, cross-electrophile coupling, and the use of semiconductor nanomaterials in photochemical reactions.

2. Sacrificial Anodes

2.1. Aryl–Aryl

Despite the challenges inherent in a cross-Ullman coupling of two aryl electrophiles, several groups have developed conditions that give cross-selectivity with certain substrate pairs. Navarro and co-workers demonstrated the Ni-catalyzed dimerization of bromo-pyridines and the heterocoupling of bromo-pyridines using a sacrificial Zn or Fe anode, Ni foam cathode, NaI as the electrolyte, and DMF as the solvent in an undivided cell at room temperature (Figure 2).[15] Ligand was not added as the product could act as a ligand. The reactions proceeded under constant current (100 mA, 4.76 mA/cm^2). A pre-electrolysis period with 1,2-dibromoethane and electrolyte in solvent was used to generate iron ions in solution before adding the catalyst and reagents. An iron anode provided higher yields than a zinc anode due to the iron ions being better at trapping the bipyridine (bpy) product to limit passivation of the Ni catalyst. Statistical yields (2:1:1 cross-product/dimer/dimer) were obtained for the heterocoupling reactions. Homocoupling of 2,6-dihalopyridines required Ni(bpy)Br$_2$ as the catalyst since the product did not act as a sufficient ligand. There was a large amount of bpy formed, possibly from direct reduction of the dihalogenated product at the cathode. They determined that using a Zn anode instead of Fe increased the formation of the desired product versus bpy. They were also able to form terpyridines from 2,6-dichloropyridine and 2-bromo-6-methylpyridine, albeit at low yields using a Zn anode and Ni(bpy)Br$_2$ as the catalyst.

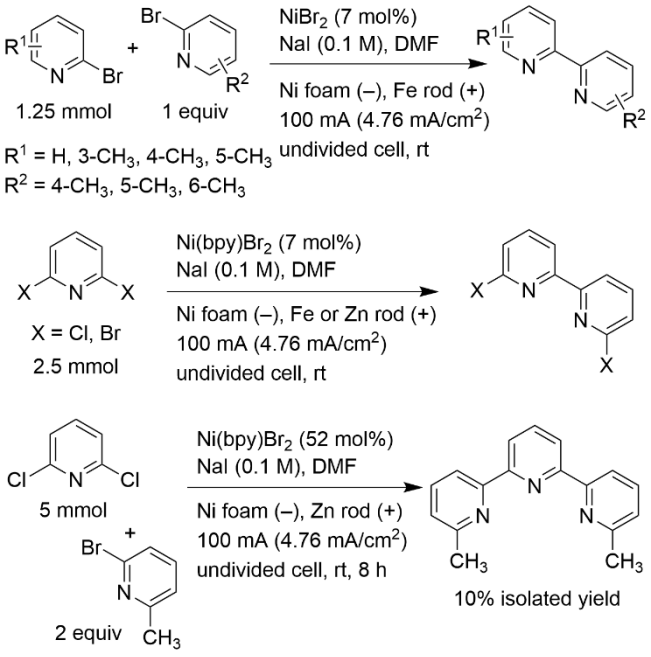

Figure 2. Pyridine dimerization and cross-coupling by Navarro and co-workers.

Le Gall, Léonel, and co-workers coupled 4-amino-6-chloropyrimidines with aryl iodides and bromides using an Fe anode and Ni foam cathode in an undivided cell (Figure 3).[16] They used Ni(bpy)Br$_2$ as the catalyst and tetrabutylammonium bromide (TBABr) as the electrolyte. A pre-electrolysis period with 1,2-dibromoethane and electrolyte in solvent was used to form iron salts. Then the catalyst and substrates were added, and constant current electrolysis (200 mA) was applied. Aryl iodides were used for substrates with electron-donating or -neutral groups. Aryl substrates with ortho substituents showed a decrease in yield. Chloropyrimidines substituted with an aromatic amine rapidly dimerized and thus had low yields of cross-product. A chloropyrimidine with an unprotected N-H substituent was tolerated.

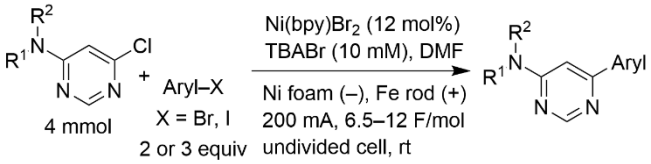

Figure 3. Coupling of pyrimidines with aryls by Le Gall, Léonel, and co-workers. X = I or Br.

In a follow-up paper, Le Gall, Léonel, and co-workers showcased the coupling of 4-chloro-6-pyrrolylpyrimidines with (hetero)aryl iodides/bromides (Figure 4).[17] In a comparison to Suzuki–Miyaura conditions with Pd-catalyzed coupling of 4-chloro-6-pyrrolylpyrimidine and Aryl-B(OH)$_2$, the Ni-catalyzed reductive electrochemical conditions show similar or higher yields.

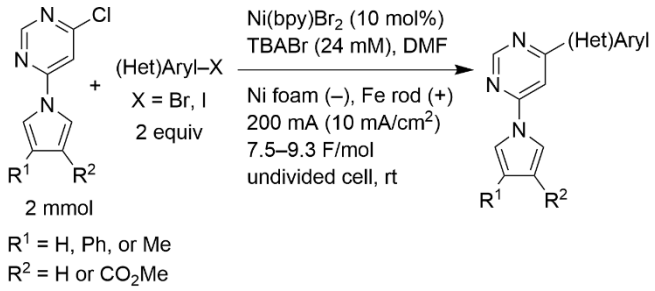

Figure 4. Coupling of pyrimidines with (hetero)aryls by Le Gall, Léonel, and co-workers.

Another paper by Léonel and co-workers reported the coupling of 3-amino-6-chloropyridazines with (hetero)aryl iodides/bromides using an Fe/Ni anode and Ni foam cathode in an undivided cell (Figure 5).[18] The reaction is catalyzed by $Ni(bpy)Br_2$ under constant current (200 mA, 10 mA/cm^2). As in the previous examples, a pre-electrolysis period with 1,2-dibromoethane and electrolyte in solvent was used to generate metal salts in solution. The nickel salts generated from the anode were beneficial to the reaction yield as compared to having an Fe only anode. They demonstrated that the electrochemical method using Aryl-I/Br provided higher yields compared to Pd-catalyzed Suzuki ($ArylB(OH)_2$) and Stille ($ArylSnBu_3$) couplings.

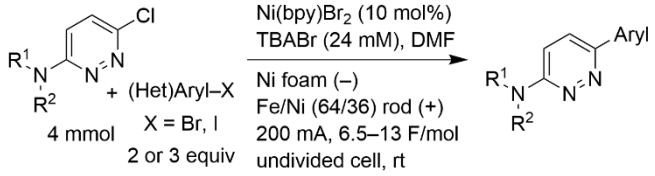

Figure 5. Coupling of amino-pyridazines with (hetero)aryls by Léonel and co-workers.

In a follow-up paper using the same conditions, Léonel and co-workers expanded the scope of chloropyridazines and aryl iodides/bromides (Figure 6).[19] These 3-amino-, 3-aryloxy- and 3-alkoxy-6-(hetero)arylpyridazines were evaluated in cancer cell lines for use as anti-tumor agents.

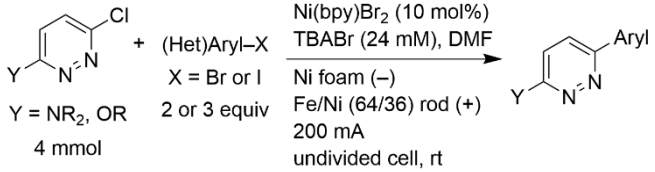

Figure 6. Coupling of amino-, alkoxy-, and aryloxy-pyridazines with (hetero)aryls by Léonel and co-workers.

Segmany, Léonel, and co-workers dimerized (hetero)aryl halides with a Fe/Ni (64:36) anode, Ni foam cathode, and $Ni(bpy)Br_2$ catalyst under constant current (200 mA, 5 mA/cm^2) in an undivided cell (Figure 7).[20] For aryl halides, NaI as the electrolyte and DMF as the solvent was used. For heteroaryl halides, they found that LiCl in DMF/pyridine (9:1) provided higher yields. Again, pre-electrolysis with 1,2-dibromoethane and electrolyte in solvent provided iron and nickel salts in solution before the catalyst and substrates were added.

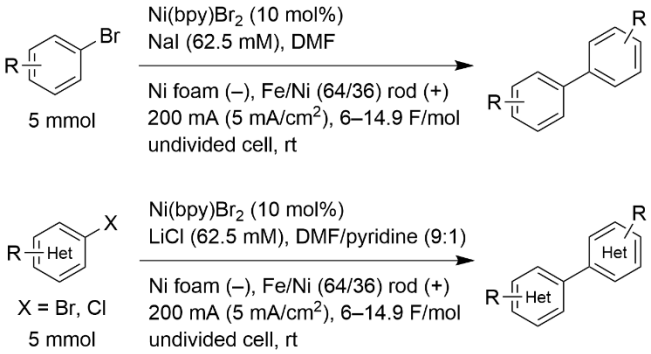

Figure 7. (Hetero)aryl dimerization by Segmany, Léonel, and co-workers.

Mei and co-workers showcased an enantioselective dimerization of aryl bromides using an Fe anode and Ni foam cathode under constant current (12 mA, 0.75 mA/cm^2) in an undivided cell at 0 °C (Figure 8).[21] When either Pt or Zn was used as the anode, little to no yield of the desired product was obtained. For Zn, mostly the protodehalogenated product was obtained. Using an Fe anode greatly improved the selectivity towards the dimer. Using $NiCl_2$•glyme and an indane-fused oxazoline ligand, they synthesized axially chiral BINOL derivatives, including 3,3′-diaryl BINOLs. They demonstrated higher yields with the electrochemical method compared to using Mn dust as the reductant.

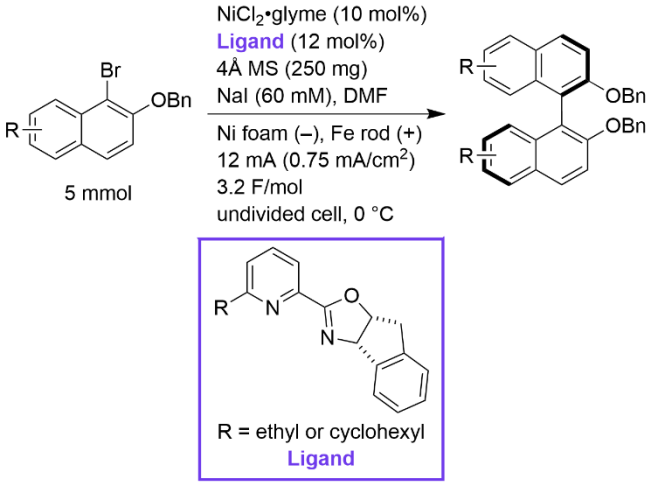

Figure 8. Enantioselective dimerization of aryls by Mei and co-workers.

In a follow-up paper, Mei and co-workers demonstrated the coupling of dihaloaryls to synthesize triphenylenes using an Fe anode and Ni foam cathode under constant current (6 mA, 1 mA/cm^2) in an undivided cell (Figure 9).[22] Without electrolysis, neither Mn, Zn, nor Fe powder were effective reductants. They propose that the reaction involves a benzyne intermediate. Finally, use of 2,2'-di-iodo-biphenyls allowed for cross-coupling.

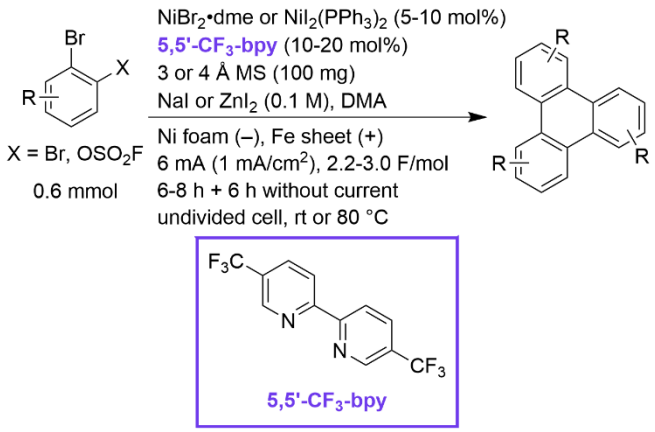

Figure 9. Trimerization of aryls by Mei and co-workers.

Beckham, Stahl, and co-workers coupled lignan-derived aryl pseudo-halides under constant potential which can then be turned into greener, better-performing plasticizers for poly(vinyl chloride) (PVC) (Figure 10).[23] Non-electrochemical high throughput screening with Zn reductant allowed for rapid ligand optimization which was then translated to an electrochemical method. Aryl mesylates could be homocoupled using bpy as the ligand, LiBr as the electrolyte with a Mg anode in a divided cell. For an aryl triflate with two ortho methoxy groups, a diphosphine ligand (DPEPhos) was used, the electrolyte was changed to LiCl, and DMSO was used as the solvent with a SS anode in an undivided cell. To obtain better selectivity for cross-coupled products, a Pd cocatalyst was employed with $ZnCl_2$ to promote transmetalation between Ni and Pd. For all these reactions, the potential was set using a reference electrode ($Ag/AgNO_3$) allowing for better reproducibility than constant cell potential which is influenced by the setup. The homocoupling of methyl 4-mesylatebenzoate was scaled up (48 mmol) in flow with 2 mol% catalyst loading and retained high yield.

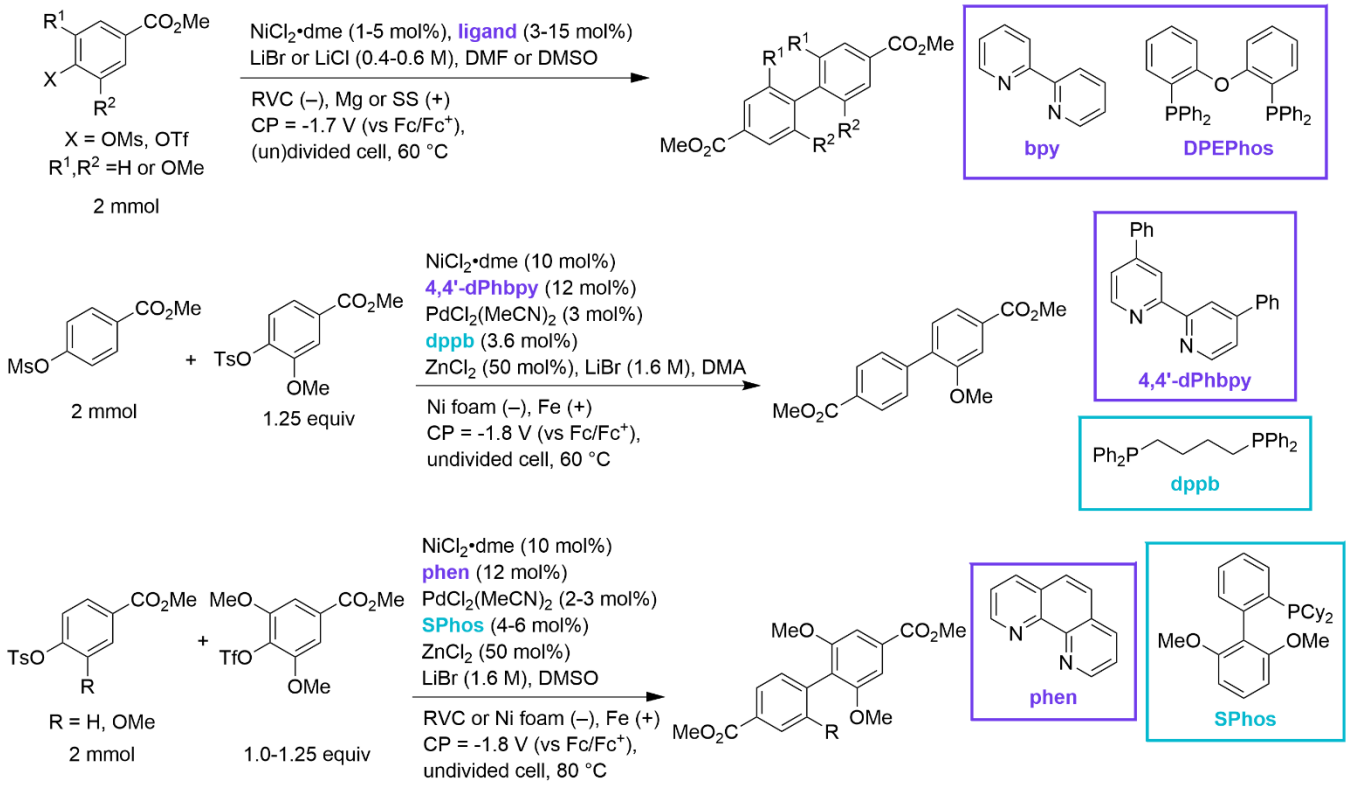

Figure 10. Dimerization and cross-coupling of lignan-derived aryl pseudo-halides by Beckham, Stahl, and co-workers.

2.2. Aryl–Alkenyl

Walker and Sevov demonstrated a Ni-catalyzed Mizoroki−Heck coupling of aryl bromides with activated and unactivated alkenes using an Fe anode and Ni foam cathode in an undivided cell at 70 °C, under constant current (varies depending on the substrates, 3–9 mA, 1.6–4.7 mA/cm^2) (Figure 11).[24] Although the Heck reaction is redox neutral, migratory insertion and turnover of nickel in Heck reactions is a challenge.[25,26] This system appears to avoid these challenges by reducing less reactive arylnickel(II) to a more reactive arylnickel(I) and then mediating turnover through a series of steps involving further reduction. The Fe anode performed better than a Zn anode, which suffered from high cell voltage (perhaps due to passivation). Styrene derivatives are obtained with a 3:1 ratio or higher of linear to branched products and allylic products were obtained from cyclic alkenes. When ethyl acrylate is used, further reduction leads to the formation of only the alkyl product. Scaling to 4.5 mmol is demonstrated.

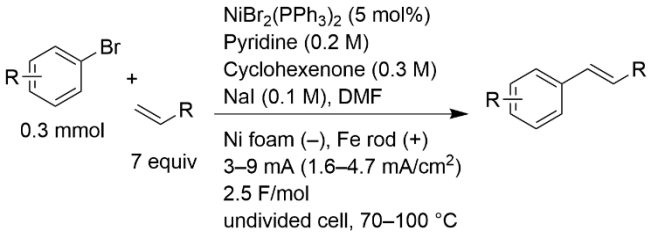

Figure 11. Coupling of aryl bromides with alkenes by Walker and Sevov.

2.3. Aryl–Alkyl

Building upon earlier studies on electrochemically-driven cross-electrophile coupling using sacrificial anodes,[27] Perkins, Hansen and co-workers demonstrated the coupling of (hetero)aryl bromides with alkyl bromides using a Zn anode and RVC cathode in an undivided cell under constant current (varies depending on the substrates, 1.5–10 mA, 1.5–10 mA/cm^3) (Figure 12).[28] NaI served a dual role as the electrolyte and an additive to activate the alkyl bromide (as the alkyl iodide via halide exchange).[29] Although Al and Mg anodes were ineffective, an Fe anode worked, albeit in slightly lower yield than Zn. Raising the temperature from ambient to 65 °C allowed for higher Faradaic efficiency. The conditions were compatible with a wide variety of catalysts based upon bipyridine, pyridine carboxamidine, and pyridine bis(carboxamidine). The electrochemical method was competitive with using Zn powder as the reductant, notably providing higher yields with substrates that directly reacted with Zn powder, such as bromo-pyrimidine or bromo-pyrazole.

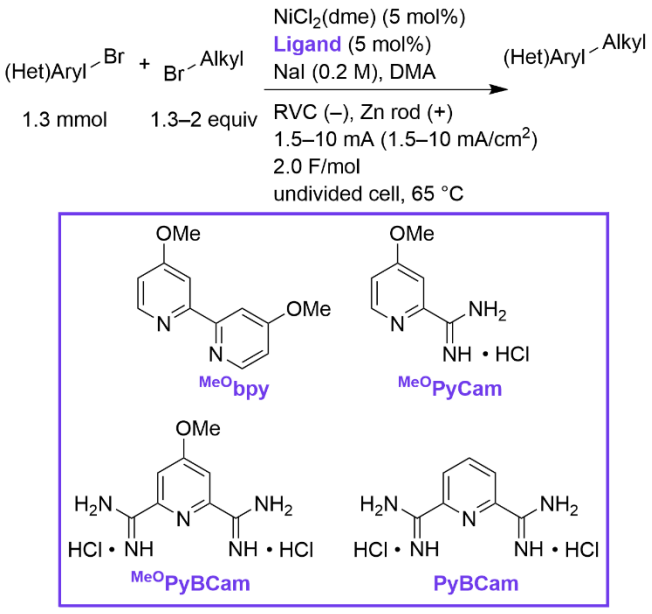

Figure 12. Coupling of (hetero)aryl bromides with alkyl bromides by Hansen and co-workers.

Loren and co-workers adapted these conditions to the coupling of aryl iodides with in-situ generated *N*-hydroxyphthalimide (NHP) esters (Figure 13)[30] based on the non-electrochemical method.[31] The conditions used a Zn anode and RVC cathode in an undivided cell under constant current (3 mA). Mg and Al anodes allowed for some product formation, although significantly lower than with a Zn anode. Using their optimized conditions, a wide variety of aryl iodides could be coupled with primary and secondary alkyl carboxylates. Limitations were electron-rich aryl iodides, tertiary alkyl carboxylates, and cyclopropyl carboxylates (the latter require different conditions, vide infra, Figure 18).[32]

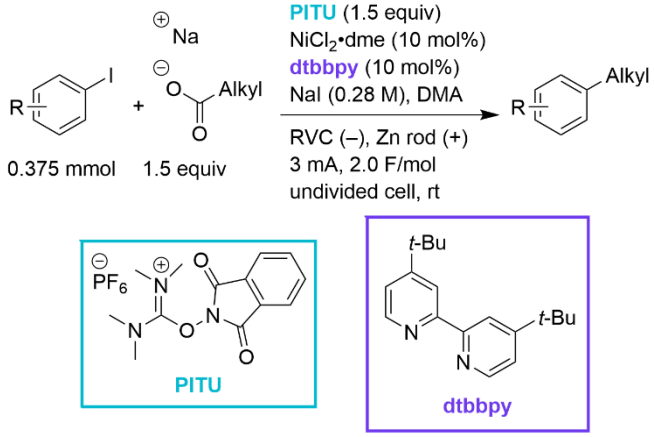

Figure 13. Coupling of aryls iodides with alkyl carboxylates by Loren and co-workers.

A challenge for some electrochemically-driven cross-electrophile coupling reactions is over-reduction of the catalyst. Sevov and co-workers explored the use of an "overcharge protector" in the coupling of (hetero)aryl bromides with alkyl bromides using a Zn anode and Ni foam cathode in an undivided cell under constant current (varies depending on the substrates, 0.5–3 mA, 0.26–1.56 mA/cm^2) (Figure 14).[33] The catalyst and the overcharge protector utilized the same ligand, bis(pyridylamino)isoindoline (MeBPI), simplifying the setup. In some cases, catalytic PPh_3 was added. Overall, the scope was broad, encompassing aryl, heteroaryl, and vinyl halides. Notably, the reaction was scaled up to 75 mmol (decagram scale).

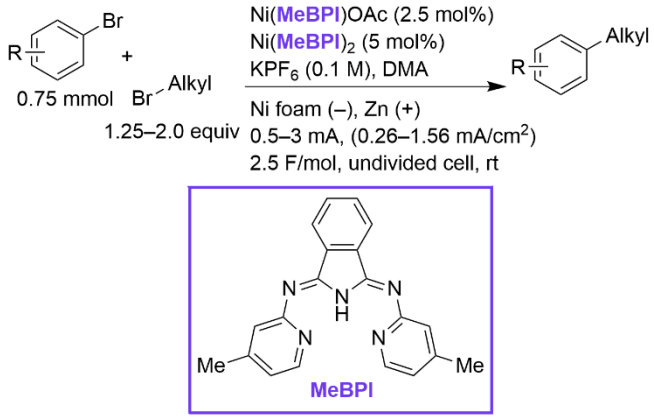

Figure 14. Coupling of (hetero)aryl bromides with alkyl bromides by Sevov and co-workers.

Continuing their work, Sevov and co-workers demonstrated other catalyst and mediator pairings for the coupling of (heteroaryl)bromides with alkyl bromides

(Figure 15).[34] Improvement in the selectivity was demonstrated for electron rich aryl bromides and heteroaryl bromides without further optimization (e.g., current density, alkyl bromide equivalences).

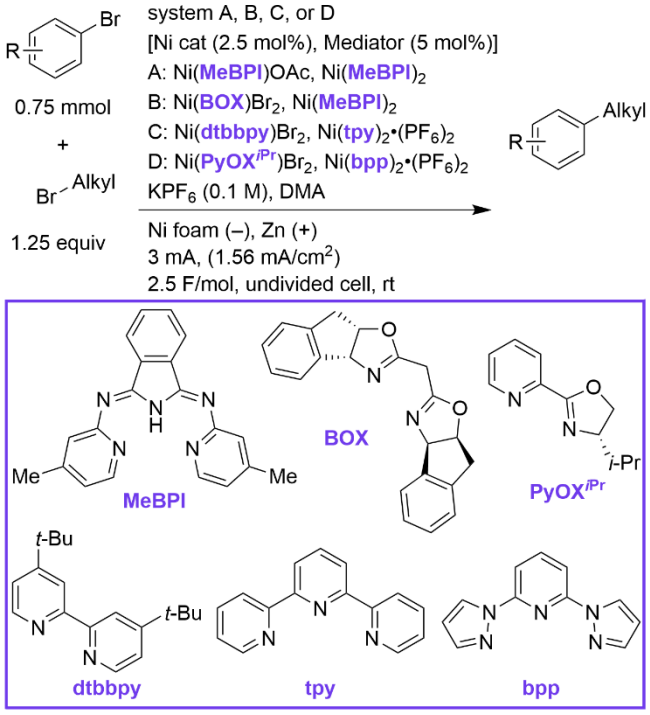

Figure 15. Coupling of (hetero)aryl bromides with alkyl bromides with new catalyst/mediator pairings by Sevov and co-workers.

Scalability was a primary concern in a recent study by Beutner, Simmons, and co-workers at BMS that examined various methods, including electrochemistry, to couple 5-bromo-3-isopropyl-1*H*-indole with *N*-Boc-4-bromopiperidine (Figure 16).[35] Notably, various electrolytes and solvents were examined in an undivided cell under constant current electrolysis with a Zn anode and RVC cathode. High conversion and selectivity were obtained with TBABr in DMA, acetone, and 2-butanone, as well as NaBr in DMA. High conversion, but low selectivity, was observed with TBAI in DMA. Poor results were obtained with tetramethylammonium bromide (TMABr) and $TBAPF_6$ in DMA and with TBABr in MeCN, isopropanol, and methyl isobutyl ketone. For electrode material, lower conversion was observed with graphite as the cathode vs RVC. Among anode materials, Al and Mg showed low conversion, Fe and Ti had good conversion with slightly lower selectivity, and SS had very low selectivity. A 5 mmol scale up demonstrated that DMA provided the highest isolated yield.

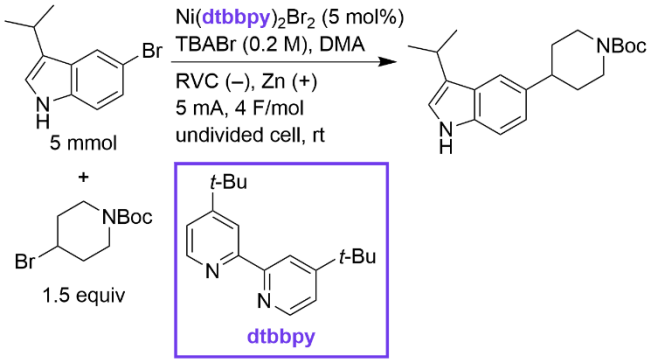

Figure 16. Coupling of 5-bromo-indole with *N*-Boc-4-bromopiperidine by Beutner, Simmons, and co-workers.

A Merck team led by Montero Bastidas and El Marrouni compared photo- and electro-chemical conditions to form tedizolid analogues (Figure 17).[36] The reaction was optimized using a high throughput electrochemical reactor with sacrificial Zn anodes. Notably, applying constant cell voltage resulted in higher yield than constant current. Based on cheminformatics, a variety of commercially available alkyl bromides were selected to compare the scope of both methods.

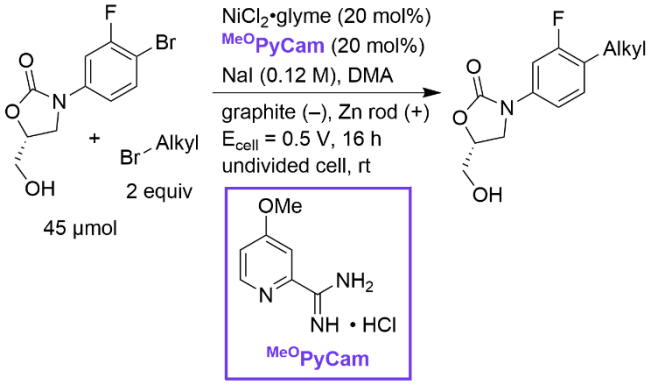

Figure 17. Coupling of the tedizolid core with alkyl bromides by Montero Bastidas, El Marrouni, and co-workers.

Baran and co-workers, in collaboration with a number of industrial researchers, adapted the silver-doped anode conditions developed for the coupling of vinyl iodides with NHP esters[37] (vide infra, Figure 27) to the coupling of NHP esters with a variety of aryl halides (Figure 18).[32] As with the vinyl iodides, a broad scope is reported. Notably, these reactions could be set up under air using NHP esters prepared in-situ. On small scales, added electrolyte was not necessary, but on larger scales LiCl was utilized. The chemistry was scaled down to 50 µmol scale in a parallel electrochemistry setup and scaled up to decagram scale in a parallel plate flow reactor via recirculation (8.3 mmol/h, 0.069 mmol/h/cm^2).

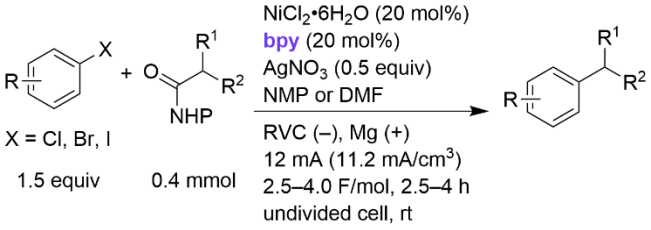

Figure 18. Coupling of aryl halides with alkyl NHP esters by Baran and co-workers.

The abundant amine substrate pool can be accessed via Katritzky salts which have previously been coupled with aryl bromides under non-electrochemical conditions by several groups.[38–42] Noël and co-workers reported the coupling of aryl iodides with secondary alkylpyridinium (Katritzky) salts under constant current electrolysis (4 mA, 2 mA/cm^2) with a sacrificial SS anode (Figure 19).[43] Primary alkyl amine-derived substrates were not tolerated.

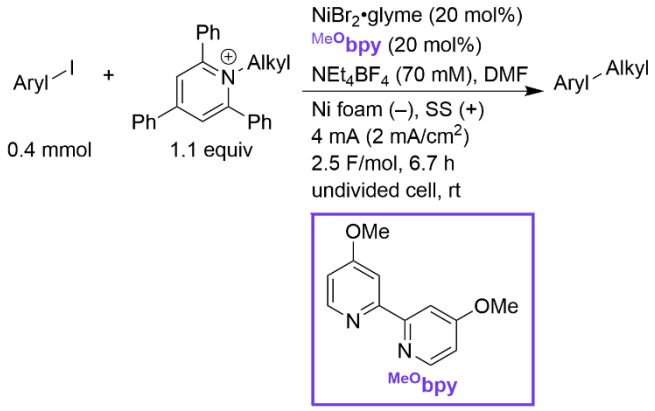

Figure 19. Coupling of aryl iodides with Katritzky salts by Noël and co-workers.

Yue, Rueping, and co-workers demonstrated the coupling of aryl iodides or alkyl acid chlorides with α-oxy halides under constant current electrolysis (8 mA, 4 mA/cm^2) with a sacrificial Fe anode (Figure 20).[44] In addition to electrocatalysis, the reaction is demonstrated via photocatalysis and with stoichiometric metal reductants by either thermal catalysis or mechanochemistry.

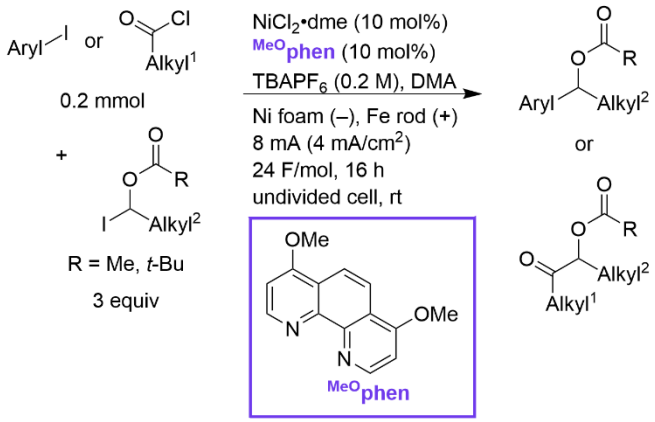

Figure 20. Coupling of aryl iodides or alkyl acid chlorides with α-oxy alkyl iodides by Yue, Rueping, and co-workers.

Complementary to the photochemical work by Doyle,[45] Qiu and co-workers reported the coupling of aryl bromides with aryl aziridines under constant current (5 mA, 2.5 mA/cm2) with a sacrificial Fe anode (Figure 21).[46] Conducting the reaction in batch at a 6 mmol scale provided slightly lower yield (80%→62%).

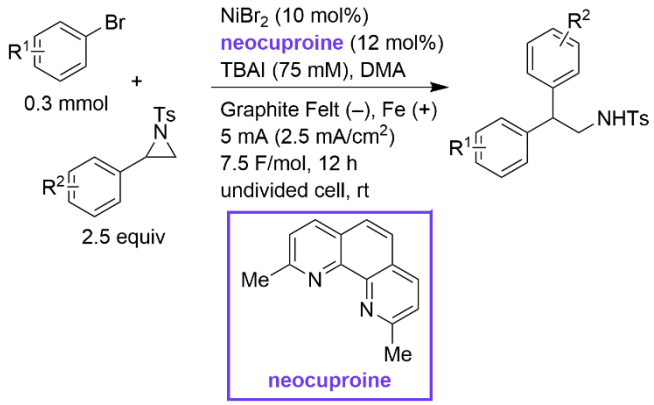

Figure 21. Coupling of aryl bromides with aryl aziridines by Qiu and co-workers.

Many of the lessons learned in the cross-electrophile coupling of alkyl halides with aryl halides can be applied to the chain-walking version of the reaction. Mei and co-workers studied the coupling of (hetero)aryl bromides and chlorides with ω-arylated alkyl bromides to form 1,1-diarylalkanes in an undivided cell equipped with an Fe anode and a Ni foam cathode under constant current (6 mA, 1.6 mA/cm^2) (Figure 22).[47] A Mg anode had significantly lower yield compared to Fe, and RVC as the cathode resulted in yields slightly lower than Ni foam. These conditions tolerated a broad substrate scope, but electron-rich aryl chlorides (no product) and secondary alkyl bromides (lower yield) were limitations. Cyclic voltammogram (CV) studies provided evidence that Ni^0 reacts with the aryl bromide in preference to the alkyl bromide.

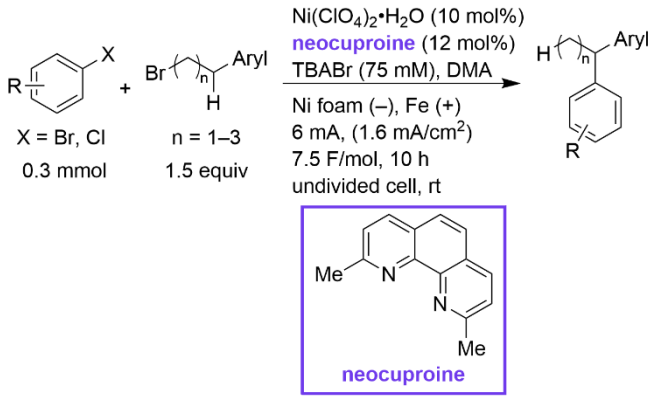

Figure 22. Coupling of (hetero)aryl bromides and chlorides with ω-arylated alkyl bromides by Mei and co-workers.

Concurrent with the Mei report, Rueping and co-workers coupled (hetero)aryl bromides with ω-arylated alkyl bromides using a stainless steel (SS 304) anode and cathode under constant current (10.5 mA, 1.5 mA/cm^2) (Figure 23).[48] A different hindered ligand (6,6'-dimethyl-2,2'-bipyridine) and electrolyte (KBr) were used. As in the Mei study, Fe (as well as SS) both worked as the anode, while Mg (plus Zn and Al) did not. This study had a particularly broad study of cathode materials: iron, brass, titanium, platinum, tin, nickel, and stainless steel worked, whereas copper, tantalum, and RVC had lower yields. Scope was broad for both coupling partners with similar limitations to the Mei study. The reaction was scaled up to 75 mmol. Hydroarylation of styrene

derivatives was also studied, requiring a higher current density (3.3 mA/cm^2) and using 1-bromopropane as the hydride source.

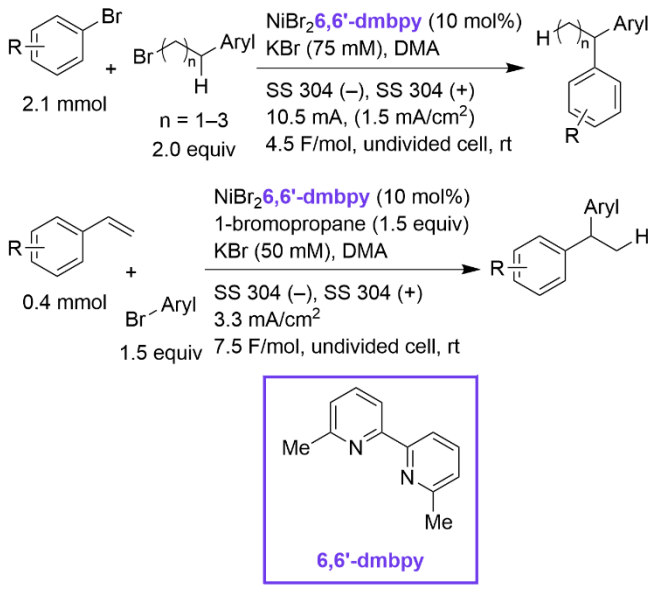

Figure 23. Coupling of (hetero)aryl bromides with ω-arylated alkyl bromides and coupling of and styrene derivatives with aryl bromides by Rueping and co-workers.

While the coupling of tertiary alkyl bromides with aryl halides has been reported by Gong using metallic reductants,[49,50] until recently there had been no electrochemical versions of this reaction. Sevov and co-workers reported a method to couple aryl bromides/chlorides/triflates or vinyl triflates with 3° and 2° alkyl bromides using a Zn anode and Ni foam cathode under constant current (varies depending on the substrates, 1–3 mA, 0.52–1.56 mA/cm^2) (Figure 24).[51] This two-catalyst system could couple challenging substrate pairs such as electron-rich aryls with 3° alkyls. This system takes advantage of the fact that Ni with a phosphine ligand is difficult to reduce electrochemically and (*i*-PrQ)Ni^0 preferentially reacts with aryl halides via a 2-electron process. In contrast, Ni with bispyrazolylpyridine (bpp) is easier to reduce and facilitates radical formation, capture, and reductive elimination. The proposed serial ligand catalysis[52] or dynamic ligand exchange[53,54] is facilitated by using Mn complexes of the bpp.

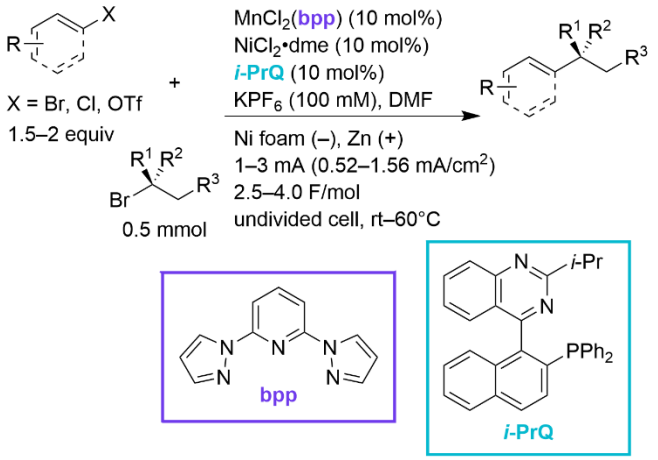

Figure 24. Coupling of aryl bromides/chlorides/triflates or vinyl triflates with 3° and 2° alkyl bromides by Sevov and co-workers.

Liu and co-workers demonstrated the coupling of (hetero)aryl chlorides with allylic sulfones under constant current (6 mA, 3 mA/cm^2) with a sacrificial SS anode (Figure 25).[55] Usually, reactions with Ni(acac)$_2$ provided higher yield than NiBr$_2$, and LiCl performed better than TBABr.

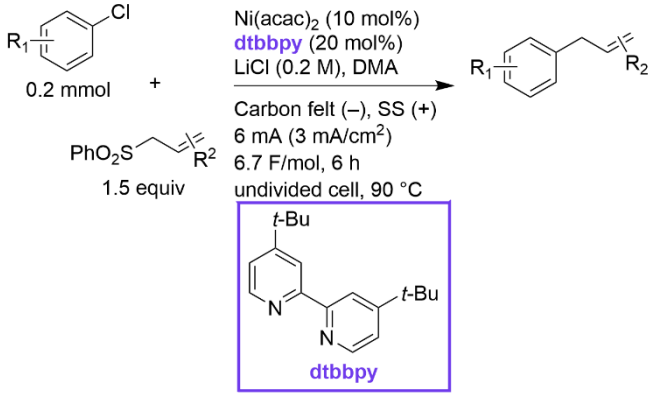

Figure 25. Coupling of aryl chlorides with allylic sulfones by Liu and co-workers.

2.4. Alkenyl–Alkyl

DeLano and Reisman reported the first enantioselective electrochemically-driven cross-electrophile coupling: the coupling of alkenyl bromides with benzylic chlorides under constant current (10 mA, 19.8 mA/cm^3) in an undivided cell using a Zn anode and RVC cathode (Figure 26).[56] Enantioselectivity was achieved using an indanyl substituted bis(oxazoline) ligand. Similar to non-enantioselective coupling reactions, RVC performed better than graphite as a cathode and a Zn anode performed better than those made of Al and Mg. An Fe anode did provide a high yield; however, it had half the Faradaic efficiency and therefore was not pursued further. Scale up of the model reaction to 6 mmol afforded high yield and ee.

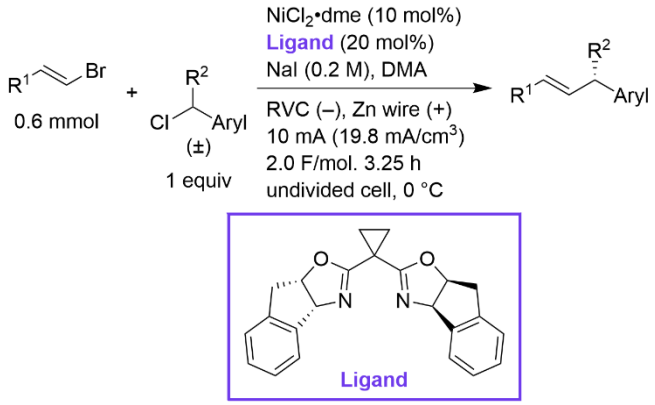

Figure 26. Enantioselective coupling of alkenyl bromides with benzylic chlorides by DeLano and Reisman.

Abruña, Anderson, Baran, and co-workers built upon the studies of Loren[30] (Figure 13) and demonstrated the cross-electrophile coupling of alkenyl iodides with alkyl NHP esters (directly or formed in-situ from carboxylic acids) in an undivided cell under constant current (6 mA, 5.6 mA/cm^3) using a Mg anode and RVC cathode (Figure 27).[37] In contrast to other studies, Zn and Fe anodes provided lower yields (as did Cu, Al, Co). Similar to previous reports, glassy carbon or graphite cathodes were significantly worse than RVC. It was found that a silver nanoparticle-modified cathode was essential for high yields because it lowers the overpotential via metal particle-analyte interactions and avoids passivation due to catalyst deposition. The method was applied to the formal or total syntheses of 13 terpenes and the chemistry was demonstrated on a 100 g scale in a flow reaction via batch recirculation (efficiency = 33 mmol/h, 0.13 mmol/h/cm^2). This work also showcased how electrochemical conditions can be tuned to a particular substrate to improve yields.

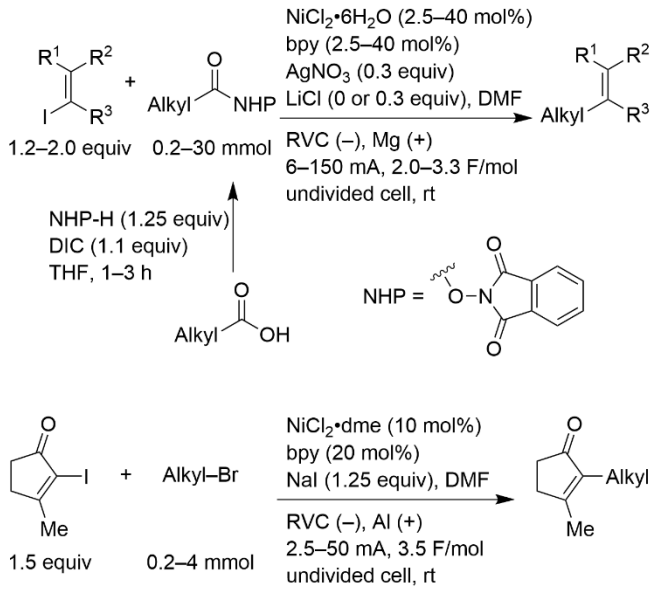

Figure 27. Coupling of alkenyl iodides with alkyl NHP esters and alkyl bromides by Abruña, Anderson, Baran, and co-workers.

Lu, Fu, and co-workers studied the coupling of trifluoromethyl alkenes with alkyl NHP esters and alkyl halides (Figure 28).[57] Constant current electrolysis (5 mA) using a sacrificial Zn anode and PyBOX as the ligand provided a variety of *gem*-difluoroalkenes.

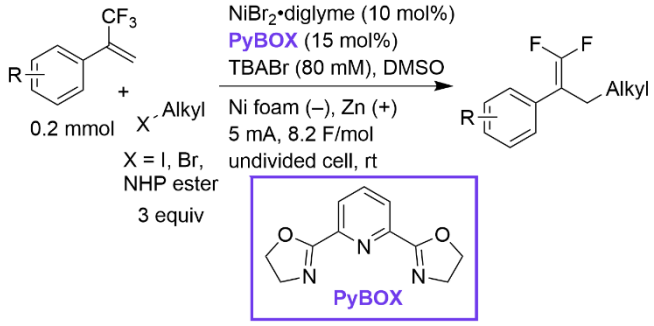

Figure 28. Coupling of trifluoromethyl alkenes with alkyl NHP esters and alkyl iodides/bromides by Lu, Fu, and co-workers.

Under similar conditions, Ni, Wang, and co-workers coupled trifluoromethyl alkenes with aryl or alkyl halides (Figure 29).[58] Differences included using tpy as the ligand and Fe as the sacrificial anode. They also expand the scope to a variety of other olefinating reagents, such as difluoroalkenes, allylic sulfones, β-hydroxy-α-methylene esters, allylic acetates, and allylic oxalates.

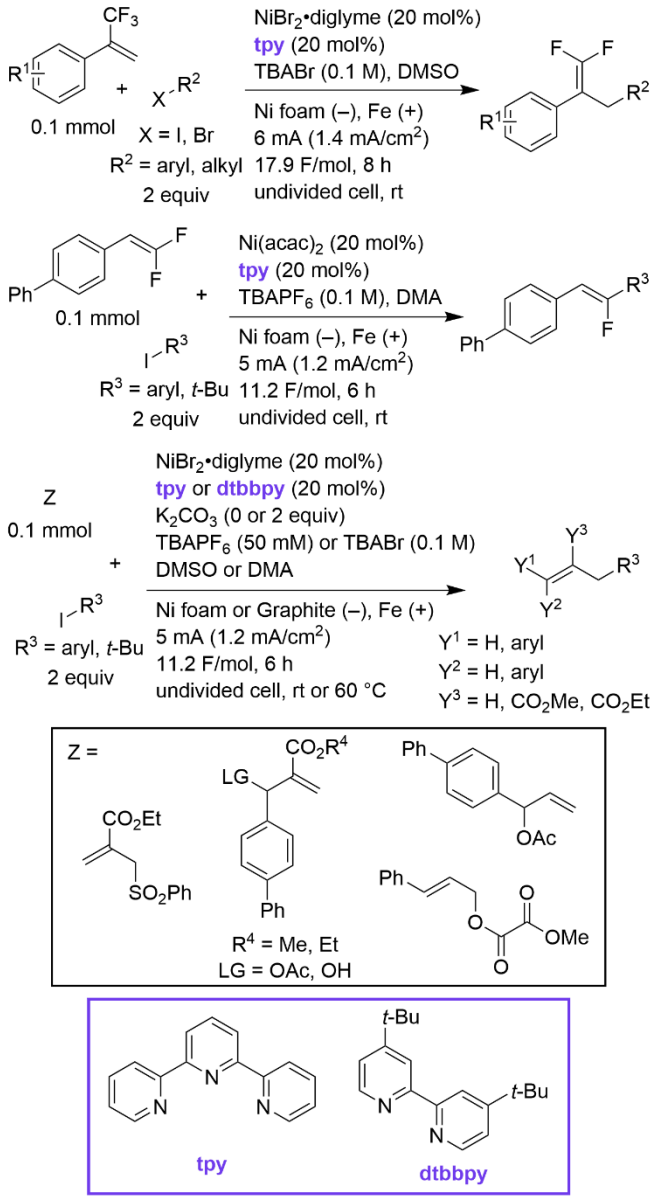

Figure 29. Coupling of trifluoromethyl alkenes, difluoroalkenes, and allylic electrophiles with aryl or alkyl halides by Ni, Wang, and co-workers.

2.5. Carbonyl–Alkyl

The coupling of activated carboxylic acids with alkyl electrophiles to form ketone products is one of the first reported highly cross-selective cross-electrophile coupling reactions and has been driven electrochemically[59–63] and with stoichiometric metals.[64–69] Building upon these studies, Yang, Xia, and co-workers reported the coupling of (hetero)aryl carboxylic acids with 2° and 1° alkyl electrophiles in an undivided cell under constant current (4 mA, 4 mA/cm^2) using an Fe anode and Ni plate cathode (Figure 30).[70] Notably, Na_2HPO_4 was used as the base and DMSO as the solvent (a rare example of a non-amide solvent). The reaction was scaled to 6 mmol with a small decrease in isolated yield (72%→58%).

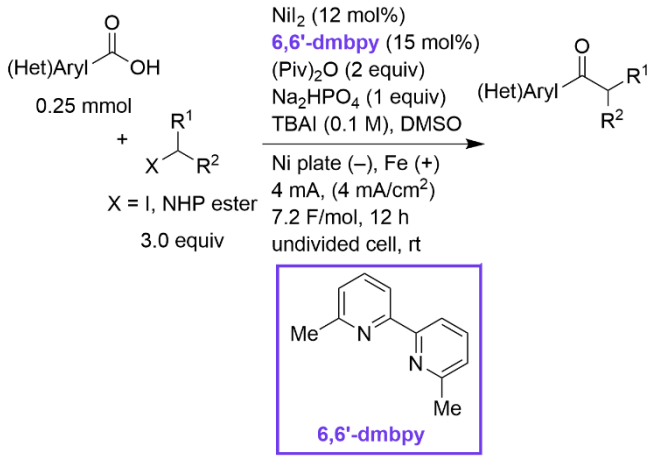

Figure 30. Coupling of aryl carboxylic acids with 2° and 1° alkyl iodides / NHP esters by Yang, Xia, and co-workers.

Vantourout, Amgoune, and co-workers demonstrated the coupling of alkyl *N*-acyl imides with alkyl bromides and benzyl chlorides at constant current (8 mA) in an undivided cell (Figure 31).[71] For anode materials, Zn worked well, but Mg did not. A Ni foam cathode provided higher yield over RVC. The authors propose that Ni^I activates both alkyl bromides and *N*-acyl imides based on CV studies. Alkyl *N*-acyl imides were also shown to react with Ni^0 in stoichiometric studies. Scaling the reaction up in batch (1 mmol) resulted in higher isolated yield (57%→80%).

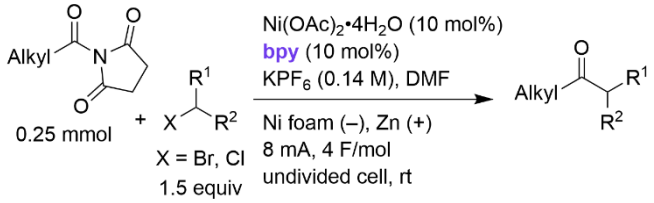

Figure 31. Coupling of alkyl *N*-acyl imides with alkyl bromides and benzyl chlorides by Vantourout, Amgoune, and co-workers.

Cheng, Mei, and co-workers were able to combine ketone synthesis with chain-walking to couple activated carboxylic acids (via a mixed anhydride) with β-aryl ethyl bromides to form α-aryl-α-methyl ketones in an undivided cell at constant current (varies depending on the substrate, 6–8 mA, 1.6–2.1 mA/cm^2) using an Fe anode and Ni foam cathode (Figure 32).[72] As has been noted previously, 6,6'-dmbpy induced chain-walking. In this case $MgBr_2$ served as the electrolyte and additive. Consistent with the related aryl and vinyl coupling reactions, an Fe anode performed better than Mg or Al and a Ni foam cathode performed better than RVC. The conditions could be extended with some success to electron-rich β-aryl ethyl bromides and γ-aryl propyl bromides.

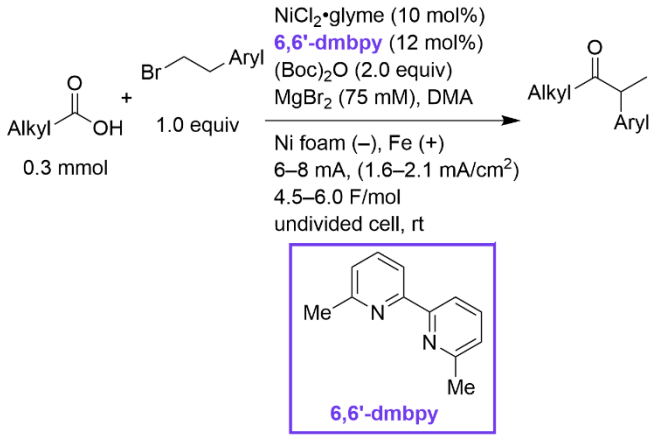

Figure **32.** Coupling of carboxylic acids with β-aryl ethyl bromides by Cheng, Mei, and co-workers.

2.6 Alkyl–Alkyl

Baran and coworkers described the doubly decarboxylative coupling of two different alkyl NHP esters to form C(sp^3)–C(sp^3) bonds (Figure 33) in an undivided cell at constant current (4 mA, 1.1 mA/cm^2).[73] Although the selectivity for cross-product over homodimeric products was lower than observed in C(sp^2)–C(sp^3) coupling reactions, reasonable yields could be obtained by utilizing an excess of one coupling partner (1.5–3 equiv). The authors demonstrated how this process could dramatically shorten syntheses. A nickel foam cathode was used along with a Zn sacrificial anode, and NaI was the supporting electrolyte. A Zn sacrificial anode was optimal, but Mg, Al, Fe, and SS all provided moderate yields (31–58% vs 72%). The optimal catalyst was a 4-methoxy-pyridine bis(oxazoline) ligand. Mechanistic studies clearly established the formation of alkyl radicals from both substrates.

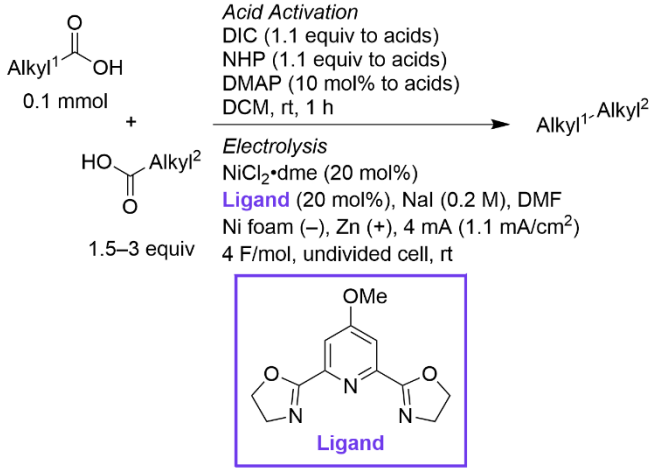

Figure 33. Cross-coupling of alkyl carboxylic acids via NHP esters by Baran and co-workers.

2.7. Other

Ackermann and co-workers described a method for C–H alkylation of unactivated 8-aminoquinoline amides using a Zn anode and Ni foam cathode under constant current (4 mA, 2.7 mA/cm^2) in an undivided cell (Figure 34).[74] Again, although this C–H alkylation is redox-neutral, access to additional oxidation and reduction steps along with the co-reduction of additional alkyl iodide allows for a faster pathway than in the non-electrochemical version. Slow addition of the alkyl iodide was required to obtain high selectivity of the cross-coupled product. Deuterium exchange experiments determined that the C–H cleavage step is irreversible and alkylzinc iodides are not an on-cycle intermediate. Instead, evidence points to alkyl radical intermediates.

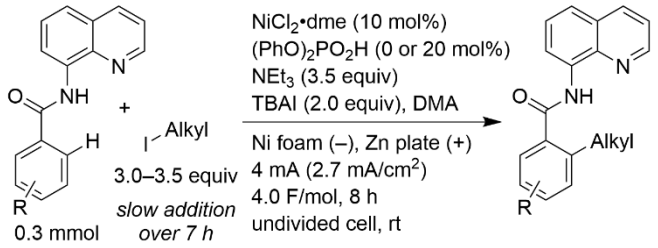

Figure 34. Coupling of 8-aminoquinoline amides with alkyl iodides by Ackermann and co-workers.

Reisman, Blackmond, Baran, and co-workers demonstrated a Nozaki−Hiyama−Kishi (NHK) coupling of alkyl aldehydes with alkenyl bromides using an Al anode and Ni foam cathode under constant cell potential (2 V) in an undivided cell (Figure 35).[75] This method expands on previous electrochemical reports on NHK couplings[76–79] and utilized the catalyst system introduced by Kishi:[80] nickel oxidative addition of the vinyl halide, transfer to chromium for addition to the aldehyde, and Cp_2ZrCl_2-mediated turnover. Constant current electrolysis provided poor results. To avoid the complication of a reference electrode, the authors utilized constant cell potential instead of constant potential. This should be less complicated in the standardized cells they used but might complicate translation to other cell designs. They also optimized an asymmetric version of the reaction, again based upon a system developed by Kishi,[81] using a chiral ligand with proton sponge to form the Cr complex in-situ, stainless steel as the anode, and MeCN as the solvent. In general, the electrochemical reactions resulted in faster rates than classical NHK coupling conditions utilizing metal powder reductants.

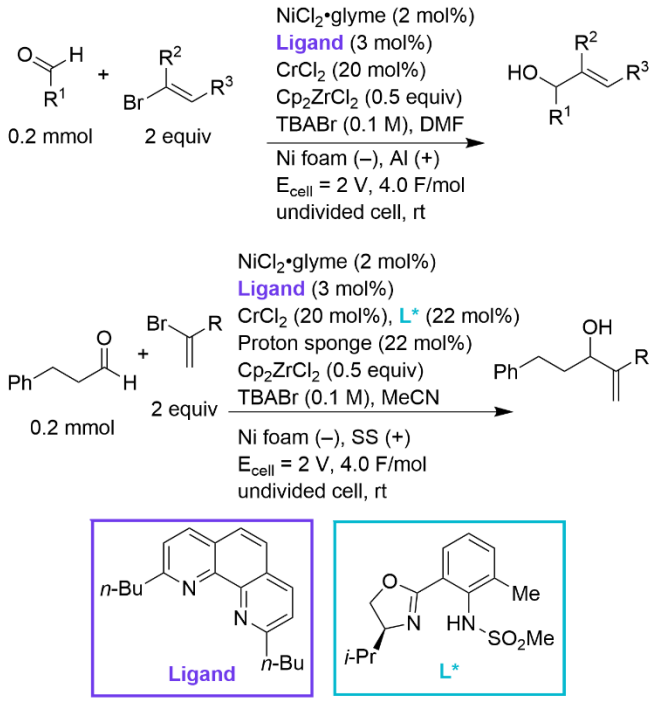

Figure 35. Coupling of alkyl aldehydes with alkenyl bromides by Reisman, Blackmond, Baran, and co-workers.

Durandetti and co-workers developed a cascade carbometalation/carbonyl addition reaction of iodoaryl alkynes with aldehydes (Figure 36).[82] Based on their previous work using stoichiometric Mn,[83] they developed an electrochemical method using an Al anode and a Ni foam cathode under constant current (25 mA, 12.5 mA/cm^2) in an undivided cell. Lower conversion and selectivity were observed with Zn or Ni anodes versus the Al anode. High yields could also be obtained at rt if the current was lowered to 15 mA and the reaction was allowed to stir for 15 min post-electrolysis. With the optimized conditions, high Faradaic efficiency was achieved and high selectivity for the *exo-dig-syn*-addition product.

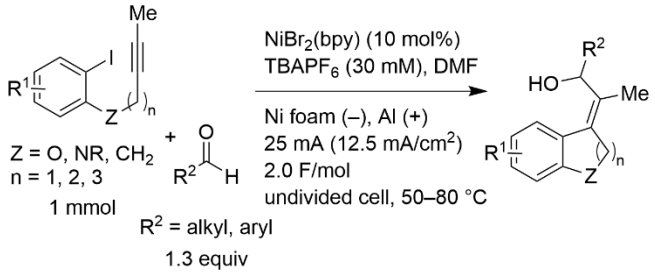

Figure 36. Cyclization of alkynyl aryl iodides and a domino reaction with aldehydes by Durandetti and co-workers.

Bai, Shi, and co-workers reported a 3-component reaction with aryl iodides, propyl chloroformate (as a CO source), and benzyl chlorides/alkyl iodides (Figure 37).[84] The reaction proceeds under constant current (15 mA, 8.3 mA/cm^2) with a sacrificial Zn anode to form alkyl aryl ketones. For alkyl iodides, a mixture of DMA/dioxane (4:2) is used and 3 equivalents of KF is added. A scale up of the batch reaction at 8 mmol maintained a relatively high yield (78%→62%).

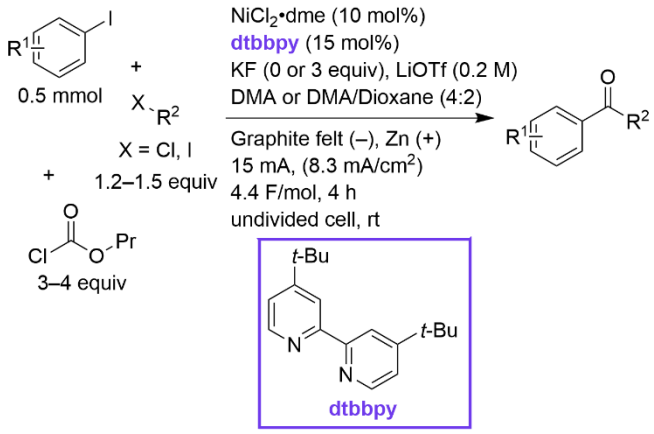

Figure 37. Coupling of aryl iodides and propyl chloroformate with benzyl chlorides/alkyl iodides by Bai, Shi, and co-workers.

3. Sacrificial Reductant

3.1 Aryl–Aryl

Perhaps the ultimate terminal reductant would be water (with oxidation to H_2O_2 or O_2 and protons). This has not been well-developed for C–C bond-forming reactions, but recently Navarro and co-workers dimerized bromopyridines using a pressed carbon powder cavity as the cathode and water as the reductant (Figure 38).[85] A 9:1 mixture of graphite powder (<20 mm) to carbon nanotubes was found to be optimal for the cathode and filter paper was used to separate the catholyte from the anolyte. They compared using constant potential (–0.8 to –1.5 V vs Ag/AgCl) and constant current (10 or 30 mA) based on product selectivity and current efficiency. Using a larger cavity cell, the reaction could be scaled up to 5 mmol. This method reduces the amount of organic solvent that is needed and eliminates stoichiometric metal waste typically produced from a sacrificial anode.

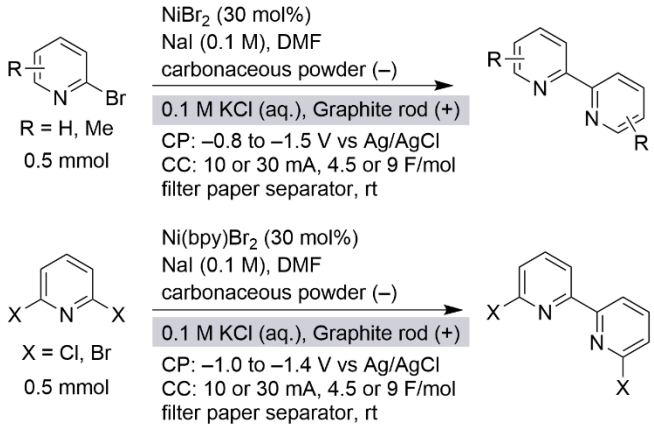

Figure 38. Dimerization of bromopyridines using a powder cavity cell by Navarro and co-workers.

3.2. Aryl–Alkyl

Jamison, Fang, Bio, and co-workers coupled (hetero)aryl iodides with alkyl NHP esters using NEt_3 as the terminal reductant in a divided cell (Figure 39).[86] This was a major advance in cross-electrophile coupling as it was the first time NHP ester cross-electrophile couplings had been run

electrochemically and the first C(sp^2)–C(sp^3) couplings accomplished without use of a sacrificial anode. RVC was used for both the cathode and anode and reactions were conducted in an H-cell (frit porosity = 10–20 μm) under constant current (20 mA, 4–4.5 mA/cm^3). In an undivided cell, minimal product is formed, and alkyl dimer is the major side product. Using Ni foam as the cathode resulted in slightly worse selectivity. A higher yield was obtained with $TBAPF_6$ as the electrolyte than with TBABr. A similar yield was observed with DIPEA as the reductant compared to NEt_3. Primary and secondary alkyls as well as adamantyl could be coupled, however, unconstrained tertiary alkyls were unable to be coupled. Using a single pass flow cell with a cation exchange membrane (Nafion) to divide the catholyte and anolyte, they observed improved selectivity towards the cross-coupled product with higher flow rates, likely due to increased mixing. Significantly higher current density (14 mA/cm^3) than batch could be achieved while maintaining or improving selectivity.

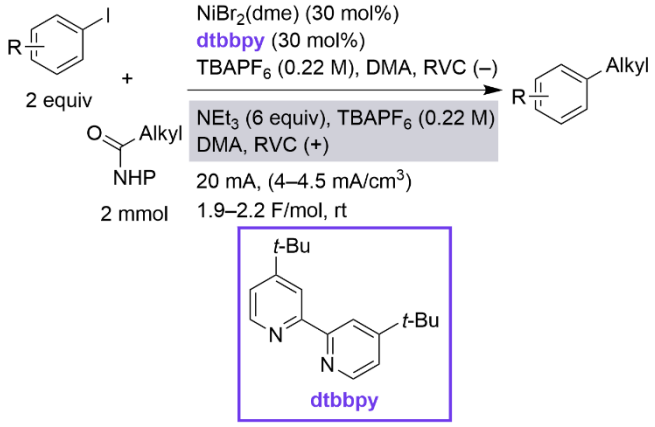

Figure 39. Coupling of (hetero)aryl iodides with alkyl NHP esters with an amine reductant by Jamison, Fang, Bio, and co-workers.

Working with our group, Perkins, Hansen and co-authors expanded on their sacrificial anode results by developing a cross-electrophile coupling of (hetero)aryl bromides with alkyl bromides using HN(*i*-Pr)$_2$ as the terminal reductant in a divided cell (Figure 40).[87] RVC was used for both the cathode and anode, however, Ni foam as the cathode also showed a similar reaction profile. A reinforced cation exchange membrane (Nafion 324) separated the cathodic chamber from the anodic chamber and a jacketed reactor filled with glycol heat transfer fluid was used to maintain elevated temperature. This method used a dual catalyst system composed of bidentate and tridentate pyridyl ligands, $TBAPF_6$ as the electrolyte, and MeCN as the solvent (notably not an amide solvent). The ratio of ligands can be tuned to achieve high selectivity based on the reactivity of the coupling partners: electron-deficient aryl substrates benefit from a higher ratio of tri-*tert*-butyl-terpyridine (ttbtpy), whereas, electron-neutral or -rich aryls benefit from a higher ratio of di-*tert*-butyl-bipyridine (dtbbpy).

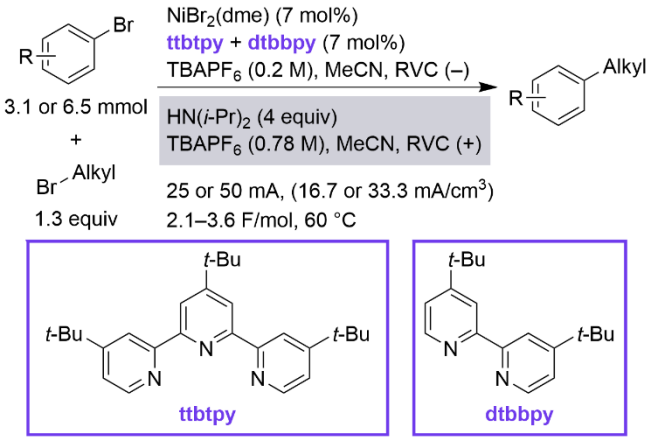

Figure 40. Coupling of (hetero)aryl bromides with alkyl bromides with an amine reductant by Hansen and co-authors.

In a follow up paper, Franke, Hansen, Weix, and co-workers demonstrated the coupling of (hetero)aryl bromides with alkyl bromides using *N*,*N*-diisopropylethylamine (DIPEA) as the terminal reductant in an undivided cell (Figure 41).[88] Ni foam was used as the cathode and graphite as the anode under constant current (10 mA, 1.3 mA/cm^2) in acetonitrile. Using the same two-catalyst system, high selectivity was obtained even with equimolar quantities of the coupling partners. We proposed that after oxidation at the anode, DIPEA forms an iminium ion followed by hydrolysis to form diisopropylamine•HBr. A comparison of scale-up approaches with parallel plate flow cells determined that batch recirculation allowed for better mixing and thus higher selectivity versus single pass. The reaction was scaled up to 12 mmol with only a slight decrease in yield, but over 4 times the current density using two flow cells connected in parallel (efficiency = 1.1 mmol/h, 0.05 mmol/h/cm^2). This method addressed concerns about metal waste, solvent greenness, and scalability, but further improvements could be envisioned (vide infra).

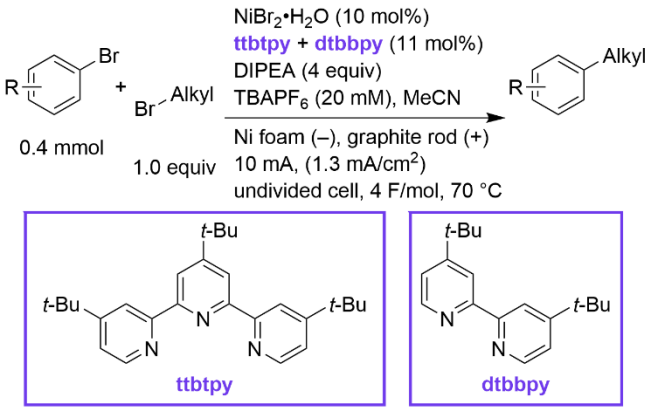

Figure 41. Coupling of (hetero)aryl bromides with alkyl bromides with an amine reductant in an undivided cell by Franke, Hansen, Weix, and co-authors.

3.3. Alkenyl–Alkyl

Budnikova and co-workers describe the coupling of fluoroalkyl iodides and bromides with alkenes using a Pt cathode and Pt anode in a divided cell (ceramic membrane)

(Figure 42).[89] There is not an added reductant, however, it is likely that DMF is oxidized in the anodic compartment. When tributyltin hydride was added, dimer formation was avoided to afford the monomer. They propose that Ni^{I} is the active catalyst based on CV analysis.

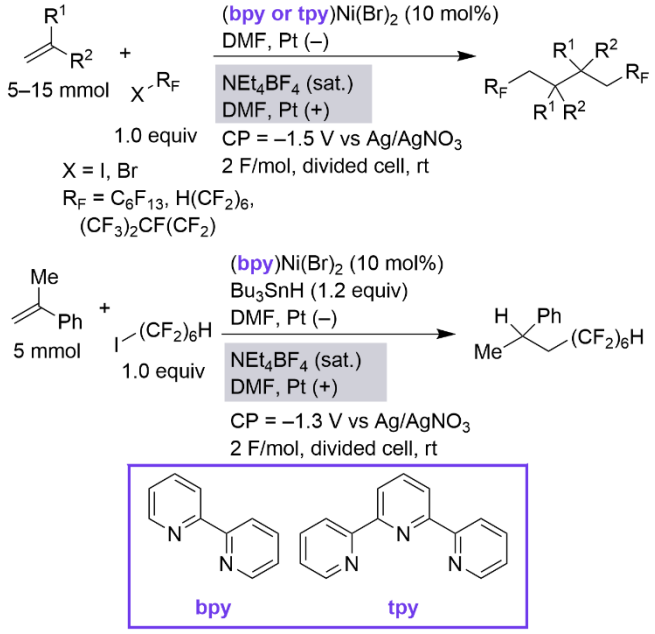

Figure 42. Coupling of alkenes with fluoroalkyl halides in a divided cell by Budnikova and co-workers.

Nevado and co-workers demonstrated an enantioselective method to couple protected aryl aziridines with alkenyl bromides using NEt_3 as the terminal reductant in an undivided cell (Figure 43).[90] Ni foam was used as the cathode and graphite as the anode under constant current (10 mA). Using the same chiral bis(oxazoline) ligand as DeLano et al.,[56] high yield and enantioselectivity was achieved. A boost in yield was observed with $MgCl_2$ as an additive. In comparison to these conditions, nonelectrochemical methods using Mn or Zn powder resulted in lower yields and decreased er. The 6 mmol scale up of the model reaction provided the product in the same er, and only a slight decrease in yield.

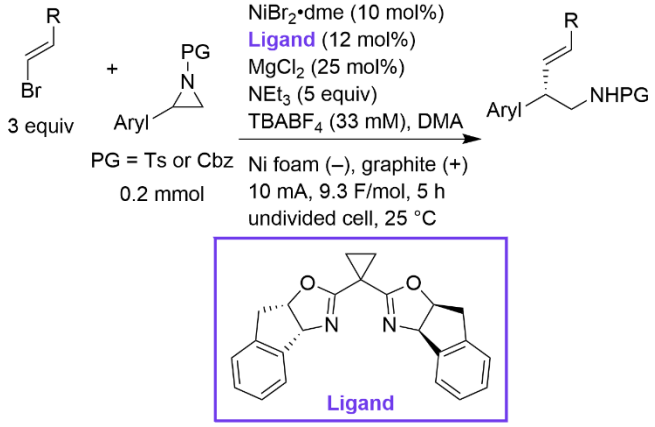

Figure 43. Enantioselective coupling of protected aryl aziridines with alkenyl bromides using an amine reductant by Nevado and co-workers.

3.4. Other

Zhu, Yue, and Rueping report a three-component stereodivergent reaction for the arylalkylation of alkynes (Figure 44).[91] Aryl bromides, alkyl bromides, and aryl alkynes were coupled together under constant current electrolysis (4 mA, 2 mA/cm^2) with *N*,*N*,*N*′,*N*′-tetramethylethylenediamine (TMEDA) as a sacrificial reductant in an undivided cell. Alkyl radical is formed via reduction of the nickel catalyst which circumvents the energy transfer process that typically occurs under photoredox conditions allowing for switching of the stereoselectivity. The *E* isomer is formed under electrolysis, whereas under photocatalysis or photo-assisted electrolysis it undergoes isomerization via energy transfer to form the *Z* isomer.

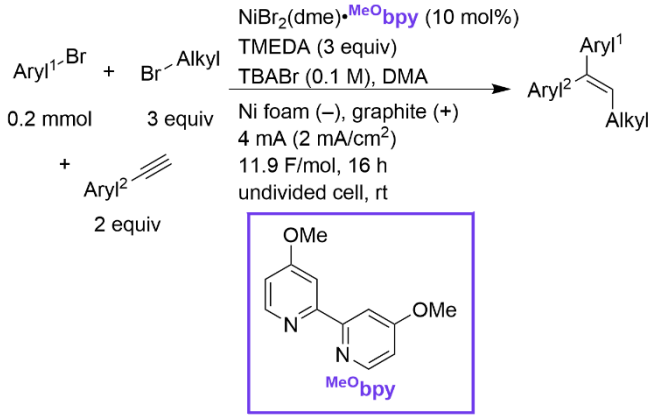

Figure 44. Arylalkylation of alkynes using an amine reductant in an undivided cell by Zhu, Yue, and Rueping.

4. Convergent Paired Electrolysis

4.1. Aryl–Alkyl

Zhang and Hu used convergent paired electrolysis to couple (hetero)aryl bromides with toluene derivatives to form diarylmethanes under constant current (3 mA, 3 mA/cm^2) (Figure 45).[92] Carbon fibre was used as the cathode, fluorine-doped tin oxide (FTO) coated glass was used as the anode, 2,6-lutidine was used as a base, and a 4:1 mixture of THF/MeCN was used as the solvent. Carbon fibre or Pt foil as the anode failed to give significant product. Linear sweep voltammetry (LSV) shows that the Ni catalyst is much more easily oxidized than 4-methylanisole at a carbon fibre surface and the reaction short circuits. However, at the surface of FTO, it is more difficult to oxidize the Ni complex, and 4-methylanisole can be oxidized and go on to form the desired product. Short circuiting still occurs, resulting in low Faradic efficiency. The authors propose that the toluene derivatives are directly oxidized at the anode rather than by a Br• mediated process.

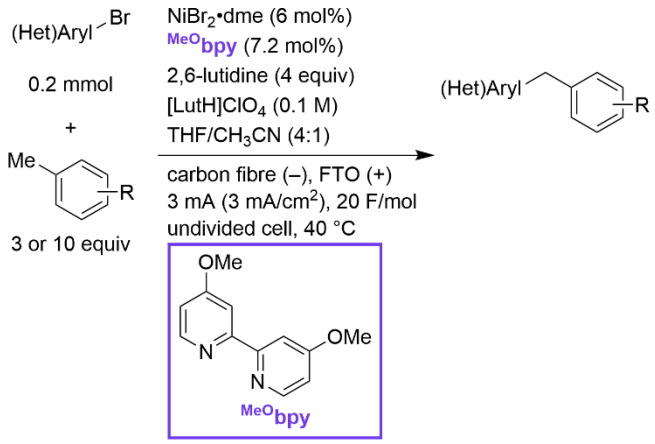

Figure 45. Coupling of (hetero)aryl bromides with toluene derivatives via convergent paired electrolysis by Zhang and Hu.

Li and co-workers reported the coupling of (hetero)aryl bromides with alkyl and π-activated alcohols under constant current (4 mA, 4 mA/cm^2) in an undivided cell (Figure 46).[93] Ni foam was used as the cathode, graphite as the anode, and LiBr as the electrolyte. PPh_3 is oxidized by Br• and reacts with alcohols to form alkyl bromides. DIPEA acts as a base for the HBr co-product of the alcohol activation process. The cross-electrophile coupling then occurs between the alkyl bromide and the aryl bromide as has been reported elsewhere. When RVC was used instead of graphite, the yield decreased significantly. The scope of the reaction is broad, including 1° and 2° (but not 3°) alcohols.

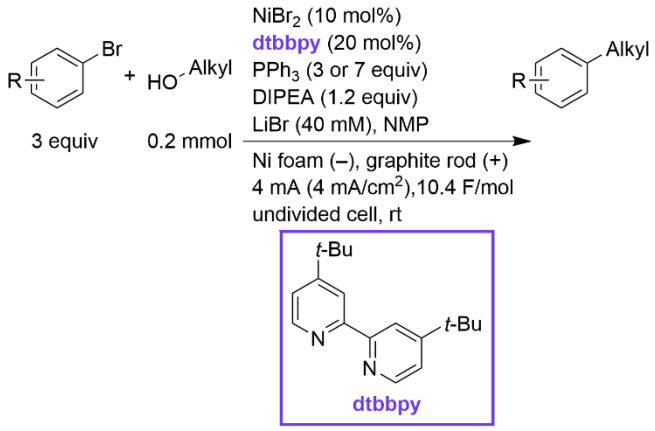

Figure 46. Coupling of (hetero)aryl bromides with alkyl and π-activated alcohols via convergent paired electrolysis by Li and co-workers.

In principle, paired electrolysis could be a replacement for photoredox catalysis. Liu and co-workers reported the coupling of (hetero)aryl bromides, aryl chlorides, or alkenyl bromides with benzylic trifluoroborates under constant current (3 mA) in an undivided cell (Figure 47).[94] This is based on a classic nickel photoredox reaction developed by Molander.[95] In the paired electrolysis, RVC was used as both the cathode and anode, K_2CO_3 was used as the base, and $LiClO_4$ was used as the electrolyte. In an undivided cell, undesired oxidation reactions can compete: 4-bromo-phenol could not be coupled as it was easier to oxidize than the benzylic trifluoroborate substrate. Scalability was demonstrated in batch (2.5 mmol) and batch recirculation flow (5–10 mmol). Their studies contained a relatively common misinterpretation of (bpy)Ni CV data: that the first reduction peak corresponds to a ($Ni^{II/I}$) when it is actually a net two-electron process ($Ni^{II/0}$);[96,97] however, the overall proposed mechanism is reasonable.

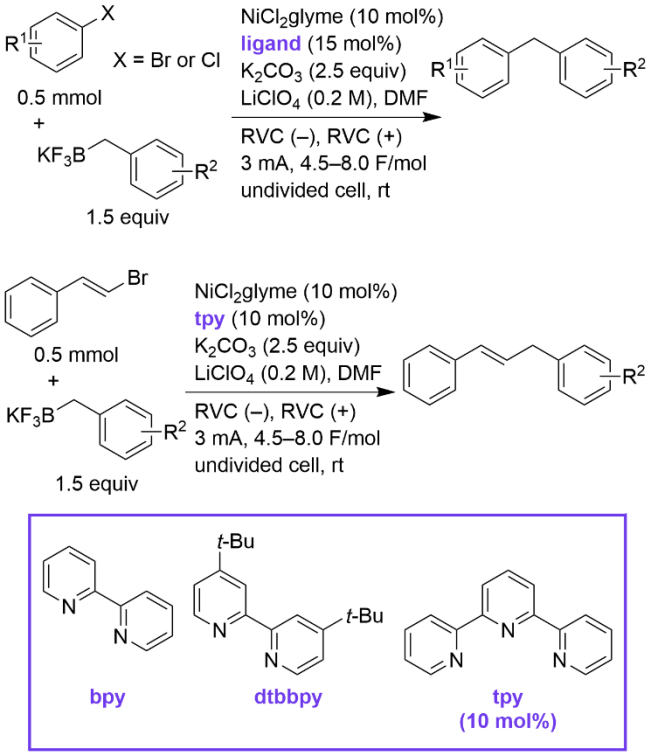

Figure 47. Coupling of (hetero)aryl bromides, aryl chlorides, or alkenyl bromides with benzylic trifluoroborates via convergent paired electrolysis by Liu and co-workers.

Zhang, Wang, and co-workers coupled (hetero)aryl iodides with sodium difluoromethanesulfinate ($NaSO_2CF_2H$) or sodium monofluoromethanesulfinate ($NaSO_2CH_2F$) under constant cell potential in an undivided cell (Figure 48).[98] For difluoromethylation, bathophenanthroline (BPhen) was used as the ligand, K_2CO_3 as a base to limit the formation of the hydrogenated byproduct, DMAP was used as a co-ligand/base, $TBABF_4$ as the electrolyte, and DMSO as the solvent. Graphite felt was used for both the cathode and anode. Platinum cathode/anode gave no product yield. Neither aryl bromides nor aryl triflates were competent coupling partners, however aryl iodides with electron donating and withdrawing groups could be coupled in good to high yields. When switching to monofluoromethylation, dtbbpy was used as the ligand instead of BPhen and moderate yields were obtained with a variety of aryl iodides. A 5.2 mmol scale batch reaction resulted in reduced isolated yield (76%→54%). Cyclic voltammetry studies determined that $NaSO_2CH_2F$ is easier to oxidize than $NaSO_2CF_2H$.

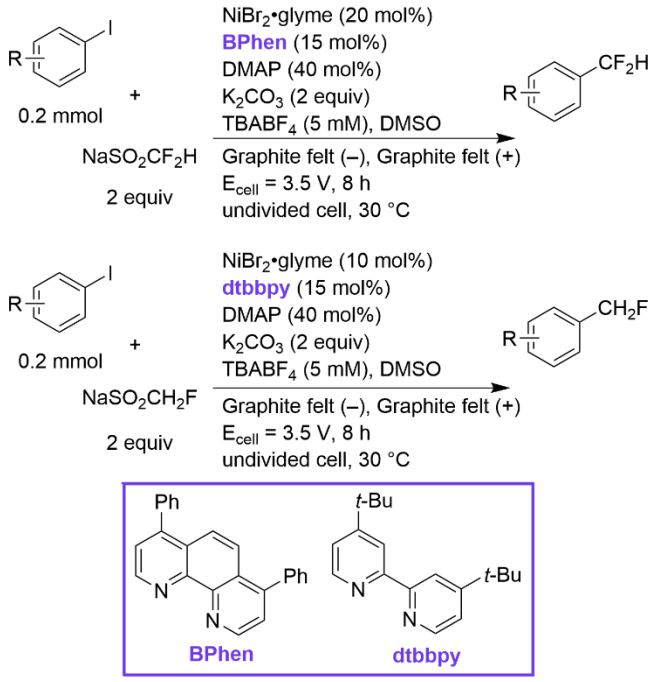

Figure 48. Couling of (hetero)aryl iodides with sodium difluoromethanesulfinate or sodium monofluoromethanesulfinate via convergent paired electrolysis by Zhang, Wang, and co-workers.

Li, Ye, and co-workers described the coupling (hetero)aryl bromides with methyl aryl amines under constant current (2 mA) (Figure 49).[99] The nickel photoredox version of this reaction was first described by Doyle, MacMillan, and coworkers.[100] In the paired electrolysis version, RVC was used as the cathode and carbon felt as the anode in an undivided cell. It is proposed that the methyl aryl amine is oxidized at the anode to form a methyl radical (after deprotonation) which can then enter the nickel catalytic cycle. While dmbpy was used as the ligand for most substrates, a few substrates worked better with tpy or 6,6'-dmbpy. Using RVC as the anode instead of carbon felt resulted in no product formation. A 10 mmol scale batch reaction maintained high isolated yield (86%→82%).

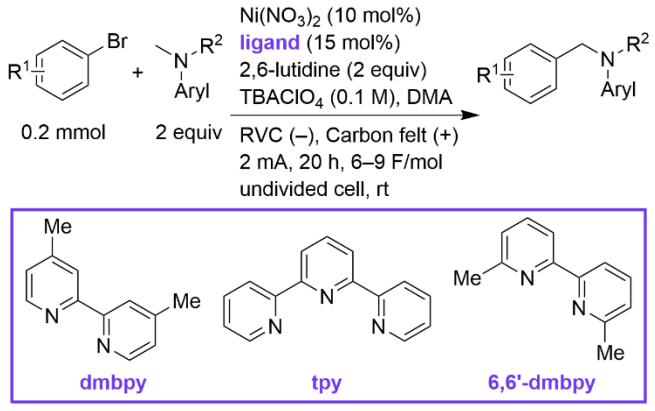

Figure 49. Coupling of (hetero)aryl bromides with methyl aryl amines via convergent paired electrolysis by Li, Ye, and co-workers.

Mei and co-workers coupled (hetero)aryl bromides with indole-3-acetic acids using constant current electrolysis (4 mA, 0.67 mA/cm^2) (Figure 50).[101] 1,8-Diazabicyclo[5.4.0]undec-7-ene (DBU) was used as a base and 2,6-lutidinium perchlorate ([LutH]ClO_4) was used as the electrolyte. The indole-3-acetic acid is deprotonated then oxidized at the anode allowing for decarboxylation and formation of a radical which can then be captured by the arylnickel intermediate.

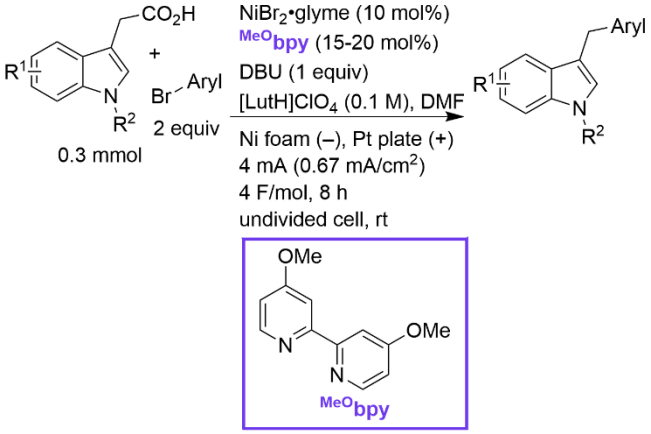

Figure 50. Coupling of indole-3-acetic acids with (hetero)aryl bromides via convergent paired electrolysis by Mei and co-workers.

Further work by Mei and co-workers includes the development of an enantioselective method to couple (hetero)aryl bromides with α-chloroesters in an undivided cell (Figure 51).[102] Tris(trimethylsilyl)silane (TTMS) was used to form the alkyl radical, in a strategy first reported by MacMillan.[103] 2,6-Lutidine was used as the base, $TBABF_4$ was the electrolyte, and a chiral bi-imidazoline (Bi-IM) was the chiral ligand. The authors propose that bromide is oxidized at the anode to a bromine radical which can form a silyl radical from TTMS. The silyl radical can form the alkyl radical from the α-chloroester by halogen atom transfer. The alkyl radical can then enter the nickel catalytic cycle and is coupled with the aryl to form the desired product. Constant cell potential (2.9 V) was found to be optimal over constant current (6 or 8 mA).

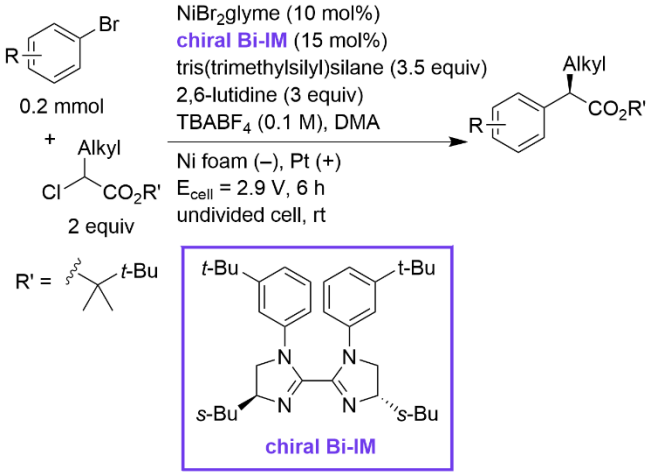

Figure 51. Enantioselective coupling of (hetero)aryl bromides with α-chloroesters via convergent paired electrolysis by Mei and co-workers.

4.2. Aryl–Carbonyl

Kong, Ni, Cao, and co-workers demonstrated the formation of ketones, amides, carboxylic acids, and aldehydes from coupling aryl trimethylammonium salts with 2-oxocarboxylic acids and derivatives under constant current (12 mA, 12 mA/cm^2) in an undivided cell (Figure 52).[104] Ni foam was used as the cathode, carbon rod as the anode, NaOAc as the base, and $TBABF_4$ as the electrolyte. A one pot procedure using *N*,*N*-dimethylaniline and MeOTf to form the trimethylammonium salts in-situ was effective with only a slight drop in yield. Two examples on 10 mmol scale in batch demonstrate the reaction is scalable. They propose the 2-oxocarboxylic acid is deprotonated by NaOAc, then oxidized at the anode, followed by decarboxylation to form an acyl radical, which is related to a strategy reported by MacMillan.[105] Mechanistic studies indicate the aryl trimethylammonium salt oxidatively adds to Ni^0.

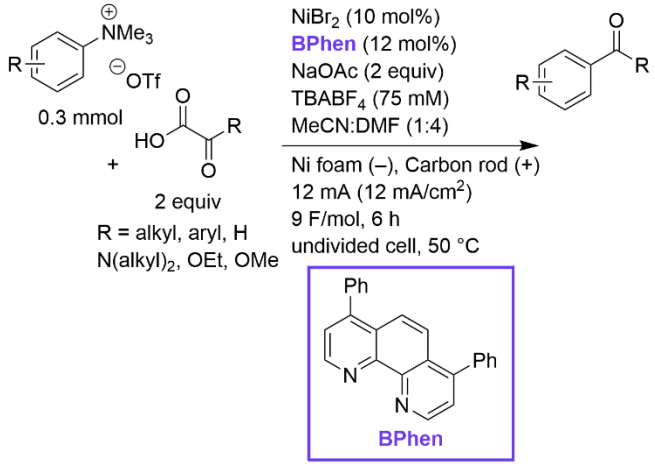

Figure 52. Coupling of aryl trimethylammonium salts with 2-oxocarboxylic acid derivatives via convergent paired electrolysis by Kong, Ni, Cao, and co-workers.

Fu and co-workers reported the coupling of (hetero)aryl bromides with methyl carbazate under constant cell potential (2 V) with a combination of Ni and Fe catalysis (Figure 53).[106] Iron(II) phthalocyanine (PcFe) mediates the formation of the alkoxycarbonyl radical at the anode. When the reaction was conducted at 4 mmol scale in batch, a drop in yield (74%→50%) was observed due to the formation of Aryl–H.

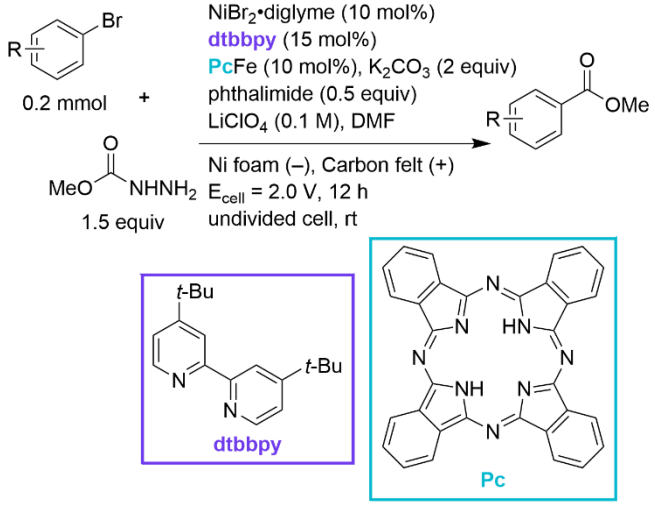

Figure 53. Coupling of (hetero)aryl bromides with methyl carbazate via convergent paired electrolysis by Fu and co-workers.

5. Outlook

The field of electrochemically-driven C–C bond formation via nickel catalysis has seen recent rapid growth that has resulted in more refined reaction methods and a broader scope of substrates that can be effectively coupled. However, opportunities remain for further advances, particularly regarding studying mechanisms and developing more efficient, green, and scalable reactions.

This survey demonstrates how most types of nickel-catalyzed C–C bond-forming reactions can be adapted to be driven electrochemically and reveals a few trends. First, the vast majority of these reactions are run in undivided cells, using a Ni or C cathode and a Zn or Fe sacrificial anode in an amide solvent. This is a sensible starting point for new chemistry because the cell design is simple and can be adapted to HTE.[107] The electrolyte used varies widely, from simple salts (NaI, MgX_2) to tetraalkylammonium salts (TBABr, $TBAPF_6$). There are several results in divided or undivided cells using amine terminal reductants, suggesting a path away from stoichiometric metal salts, but these systems appear to be less uniform. Finally, paired electrolysis has proven to be a general approach. Despite generally lower Faradaic efficiency, these reactions use simple, undivided cells and are capable of unique types of reactivity. Finally, in only a few cases have reactions been demonstrated at current densities sufficient for process-scale (≥6 mA/cm^2).[88]

Mechanistic studies are an opportunity for improving reaction rates (and current density) in nickel-mediated electrochemistry but also present a challenge. When compared to nonelectrochemical methods, differences in solvent, electrolyte, driving force, and mass-transport can impact the dominant species and mechanism in nickel-catalyzed reactions. Often, model systems that behave well electrochemically (e.g., CV shows a reversible peak) are not catalytically relevant. Despite these challenges, the answer will likely arise from the use of more electrochemistry.[6] Analytical electrochemistry offers specific advantages for nickel chemistry because many potential nickel species are both NMR and EPR silent but can be measured by electrochemical methods. In addition, design of less commonly used or new electrode materials that have different overpotentials for side reactions may help to combat short circuiting which limits Faradaic efficiency.

Electrochemistry is garnering interest due to its perceived relative environmental friendliness, but solvent is a large factor in determining the greenness of a reaction when considering scalability and use by industry. Almost all the reactions described herein are in amide solvents, and only a handful are in DMSO or MeCN. Amide solvents pose a safety and environmental concern[108] and even MeCN has some undesirable attributes.[109] Greener solvents that are compatible with electrochemistry and organic chemistry are needed. The type of electrolyte used is also an important factor. Most desirable are simple salts (MX salts), but heavier, more problematic salts are still common (e.g., $TBAPF_6$, perchlorates) because they are more soluble in less polar

solvents. In addition to safety and environmental concerns, the ideal solvent/electrolyte combination also needs to be highly conductive, solubilize the substrates and catalysts, and have a wide potential window.

For net-reductive chemistry, further improvement in generality and greenness of the terminal reductant is needed. Compared to oxidative reactions where the counter half reaction is often H^+ reduction (to form H_2), reductive reactions lack such an efficient oxidative half reaction.[110] Amine oxidation is promising, but anodic reactions that form benign/gaseous co-products would be better. For example, H_2O oxidation (to O_2 and H^+), H_2 oxidation (to H^+), formate oxidation (to CO_2 and H^+), and hydrazine oxidation (to N_2 and H^+). However, these reactions are generally optimized in water instead of organic solvents and all of them produce protons, which introduces complications for organic chemistry.

Finally, while several promising scale-up examples have been reported in this review, better flow electrochemistry cell designs are needed. Flow electrochemistry offers many potential options for tuning (mass transport, cell voltage, current density, electrode materials, divided/undivided, etc),[111,112] but this makes optimization more complicated than usual. All the examples in flow covered in this review use parallel plate reactors. Reactors that tune mass transport (either increasing or decreasing) and allow for large electrode surface areas are needed, but these more complex designs will require collaboration between organic chemists and engineers. Another area with room for innovation is membrane technology. More robust membranes and better anionic exchange membranes, made from tailored materials, could lead to significant improvements in electrochemical reactions. Finally, we have one request of researchers to facilitate improvements in the field: more detail on the electrochemical aspects of reactions. In particular, interelectrode distance, membrane product numbers (e.g., Nafion 234), electrode surface area, and total charge passed are missing from many recent studies.

The recent work summarized above offers a springboard toward improvements in electrochemical reactions with many opportunities for advancements to drive interest and implementation in industrial sectors.

Glossary

BINOL = 1,1′-Bi-2-naphthol
BPhen = 4,7-diphenyl-1,10-phenanthroline
bpp = 2,6-bispyrazolylpyridine
bpy = 2,2’-bipyridine
CV = Cyclic Voltammetry
DBU = diazabicyclo[5.4.0]undec-7-ene
DIC = *N*,*N*′-diisopropylcarbodiimide
dig = ring closure via attack on a triple bond (digonal) center
DIPEA = *N*,*N*-diisopropylethylamine (Hünig's base)
DMA = *N*,*N*-dimethylacetamide
DMAP = 4-dimethylaminopyridine
6,6’-dmbpy = 6,6’-dimethylbipyridine
dme = dimethoxyethane
DMF = *N*,*N*-dimethylformamide
DMSO = dimethylsulfoxide
DPEPhos = bis[(2-diphenylphosphino)phenyl] ether
dppb = 1,4-bis(diphenylphosphino)butane
dtbbpy = 4,4′-di-*tert*-butyl-2,2′-bipyridine
ee = enantiomeric excess
er = enantiomeric ratio
glyme = ethylene glycol dimethyl ether
(Het)Aryl = aryl or heteroaryl substrates
MeBPI = 1,3-bis(4-methylpyridyl-2-imino)-isoindoline
MeCN = acetonitrile
Neocuproine = 2,9-dimethyl-1,10-phenanthroline
NHK = Nozaki−Hiyama−Kishi
NHP = *N*-hydroxyphthalimide
NMP = *N*-methyl-2-pyrrolidone
PITU = *N*-hydroxyphthalimide tetramethyluronium hexafluorophosphate
RVC = reticulated vitreous carbon
TBA = tetrabutylammonium
TMA = tetramethylammonium
TMEDA = *N*,*N*,*N*′,*N*′-tetramethylethylenediamine
tpy = 2,2';6',2"-terpyridine
ttbtpy = 4,4′,4″-tri-*tert*-butyl-2,2′:6′,2″-terpyridine

Acknowledgements

Acknowledgements Text.

References

[1] H. Lehmkuhl, *Synthesis* **1973**, *1973*, 377–396.
[2] P. W. Jennings, D. G. Pillsbury, J. L. Hall, V. T. Brice, *J. Org. Chem.* **1976**, *41*, 719–722.
[3] E. Steckhan, *Angew. Chem. Int. Ed. Engl.* **1986**, *25*, 683–701.
[4] J.-Y. Nédélec, J. Périchon, M. Troupel, in *Electrochem. VI Electroorg. Synth. Bond Form. Anode Cathode* (Ed.: E. Steckhan), Springer, Berlin, Heidelberg, **1997**, pp. 141–173.
[5] E. Duñach, D. Franco, S. Olivero, *Eur. J. Org. Chem.* **2003**, *2003*, 1605–1622.
[6] A. Jutand, *Chem. Rev.* **2008**, *108*, 2300–2347.
[7] H. Lund, O. Hammerich, Eds. , *Organic Electrochemistry*, M. Dekker, New York, **2001**.
[8] J. Jörissen, in *Encycl. Electrochem.*, John Wiley & Sons, Ltd, **2007**.
[9] L. Yi, T. Ji, K.-Q. Chen, X.-Y. Chen, M. Rueping, *CCS Chem.* **2021**, *4*, 9–30.
[10] J. Jose, E. J. Diana, U. S. Kanchana, T. V. Mathew, *Asian J. Org. Chem.* **2023**, *12*, e202200593.
[11] S.-K. Zhang, R. C. Samanta, A. Del Vecchio, L. Ackermann, *Chem. – Eur. J.* **2020**, *26*, 10936–10947.
[12] Y. Zhang, W. Sun, C. Li, *Synthesis* **2021**, 281–294.
[13] T. R. Swaroop, M. Umashankara, V. K. Thakur, K. S. Rangappa, *J. Electrochem. Soc.* **2022**, *169*, 115501.
[14] K. Mahanty, A. Halder, D. Maiti, S. D. Sarkar, *Synthesis* **2023**, *55*, 400–416.
[15] J. L. Oliveira, M. J. Silva, T. Florêncio, K. Urgin, S. Sengmany, E. Léonel, J.-Y. Nédélec, M. Navarro, *Tetrahedron* **2012**, *68*, 2383–2390.
[16] S. Sengmany, E. Le Gall, E. Léonel, *Molecules* **2011**, *16*, 5550–5560.
[17] S. Sengmany, S. Vasseur, A. Lajnef, E. Le Gall, E. Léonel, *Eur. J. Org. Chem.* **2016**, *2016*, 4865–4871.
[18] S. Sengmany, A. Vitu-Thiebaud, E. Le Gall, S. Condon, E. Léonel, C. Thobie-Gautier, M. Pipelier, J. Lebreton, D. Dubreuil, *J. Org. Chem.* **2013**, *78*, 370–379.
[19] S. Sengmany, M. Sitter, E. Léonel, E. Le Gall, G. Loirand, T. Martens, D. Dubreuil, F. Dilasser, M. Rousselle, V. Sauzeau, J. Lebreton, M. Pipelier, R. Le Guével, *Bioorg. Med. Chem. Lett.* **2019**, *29*, 755–760.

[20] R. Rahil, S. Sengmany, E. L. Gall, E. Léonel, *Synthesis* **2018**, *50*, 146–154.
[21] H. Qiu, B. Shuai, Y.-Z. Wang, D. Liu, Y.-G. Chen, P.-S. Gao, H.-X. Ma, S. Chen, T.-S. Mei, *J. Am. Chem. Soc.* **2020**, *142*, 9872–9878.
[22] Z.-M. Li, B. Shuai, C. Ma, P. Fang, T.-S. Mei, *Chin. J. Chem.* **2022**, *40*, 2335–2344.
[23] Z.-M. Su, J. Twilton, C. B. Hoyt, F. Wang, L. Stanley, H. B. Mayes, K. Kang, D. J. Weix, G. T. Beckham, S. S. Stahl, *ACS Cent. Sci.* **2023**, *9*, 159–165.
[24] B. R. Walker, C. S. Sevov, *ACS Catal.* **2019**, *9*, 7197–7203.
[25] J. K. Vandavasi, X. Hua, H. B. Halima, S. G. Newman, *Angew. Chem. Int. Ed.* **2017**, *56*, 15441–15445.
[26] S. Bhakta, T. Ghosh, *Adv. Synth. Catal.* **2020**, *362*, 5257–5274.
[27] M. Durandetti, J. Périchon, *Synthesis* **2004**, 3079–3083.
[28] R. J. Perkins, D. J. Pedro, E. C. Hansen, *Org. Lett.* **2017**, *19*, 3755–3758.
[29] D. A. Everson, B. A. Jones, D. J. Weix, *J. Am. Chem. Soc.* **2012**, *134*, 6146–6159.
[30] T. Koyanagi, A. Herath, A. Chong, M. Ratnikov, A. Valiere, J. Chang, V. Molteni, J. Loren, *Org. Lett.* **2019**, *21*, 816–820.
[31] K. M. M. Huihui, J. A. Caputo, Z. Melchor, A. M. Olivares, A. M. Spiewak, K. A. Johnson, T. A. DiBenedetto, S. Kim, L. K. G. Ackerman, D. J. Weix, *J. Am. Chem. Soc.* **2016**, *138*, 5016–5019.
[32] M. D. Palkowitz, G. Laudadio, S. Kolb, J. Choi, M. S. Oderinde, T. E.-H. Ewing, P. N. Bolduc, T. Chen, H. Zhang, P. T. W. Cheng, B. Zhang, M. D. Mandler, V. D. Blasczak, J. M. Richter, M. R. Collins, R. L. Schioldager, M. Bravo, T. G. M. Dhar, B. Vokits, Y. Zhu, P.-G. Echeverria, M. A. Poss, S. A. Shaw, S. Clementson, N. N. Petersen, P. K. Mykhailiuk, P. S. Baran, *J. Am. Chem. Soc.* **2022**, *144*, 17709–17720.
[33] B. L. Truesdell, T. B. Hamby, C. S. Sevov, *J. Am. Chem. Soc.* **2020**, *142*, 5884–5893.
[34] J. L. S. Zackasee, S. Al Zubaydi, B. L. Truesdell, C. S. Sevov, *ACS Catal.* **2022**, *12*, 1161–1166.
[35] G. L. Beutner, E. M. Simmons, S. Ayers, C. Y. Bemis, M. J. Goldfogel, C. L. Joe, J. Marshall, S. R. Wisniewski, *J. Org. Chem.* **2021**, *86*, 10380–10396.
[36] J. R. Montero Bastidas, S. L'Heureux, W. Liu, K. Lee, A. El Marrouni, *ACS Med. Chem. Lett.* **2023**, *14*, 666–671.
[37] S. J. Harwood, M. D. Palkowitz, C. N. Gannett, P. Perez, Z. Yao, L. Sun, H. D. Abruña, S. L. Anderson, P. S. Baran, *Science* **2022**, *375*, 745–752.
[38] J. Liao, C. H. Basch, M. E. Hoerrner, M. R. Talley, B. P. Boscoe, J. W. Tucker, M. R. Garnsey, M. P. Watson, *Org. Lett.* **2019**, *21*, 2941–2946.
[39] R. Martin-Montero, V. R. Yatham, H. Yin, J. Davies, R. Martin, *Org. Lett.* **2019**, *21*, 2947–2951.
[40] S. Ni, C.-X. Li, Y. Mao, J. Han, Y. Wang, H. Yan, Y. Pan, *Sci. Adv.* **2019**, *5*, eaaw9516.
[41] J. Yi, S. O. Badir, L. M. Kammer, M. Ribagorda, G. A. Molander, *Org. Lett.* **2019**, *21*, 3346–3351.
[42] H. Yue, C. Zhu, L. Shen, Q. Geng, K. J. Hock, T. Yuan, L. Cavallo, M. Rueping, *Chem. Sci.* **2019**, *10*, 4430–4435.
[43] L. J. Wesenberg, A. Sivo, G. Vilé, T. Noël, *J. Org. Chem.* **2023**, DOI 10.1021/acs.joc.3c00859.
[44] C. Zhu, S.-C. Lee, H. Chen, H. Yue, M. Rueping, *Angew. Chem. Int. Ed.* **2022**, *61*, e202204212.
[45] T. J. Steiman, J. Liu, A. Mengiste, A. G. Doyle, *J. Am. Chem. Soc.* **2020**, *142*, 7598–7605.
[46] G. Yang, Y. Wang, Y. Qiu, *Chem. – Eur. J.* **2023**, *n/a*, e202300959.
[47] K.-J. Jiao, D. Liu, H.-X. Ma, H. Qiu, P. Fang, T.-S. Mei, *Angew. Chem. Int. Ed.* **2020**, *59*, 6520–6524.
[48] G. S. Kumar, A. Peshkov, A. Brzozowska, P. Nikolaienko, C. Zhu, M. Rueping, *Angew. Chem. Int. Ed.* **2020**, *59*, 6513–6519.
[49] X. Wang, S. Wang, W. Xue, H. Gong, *J. Am. Chem. Soc.* **2015**, *137*, 11562–11565.
[50] X. Wang, G. Ma, Y. Peng, C. E. Pitsch, B. J. Moll, T. D. Ly, X. Wang, H. Gong, *J. Am. Chem. Soc.* **2018**, *140*, 14490–14497.
[51] T. B. Hamby, M. J. LaLama, C. S. Sevov, *Science* **2022**, *376*, 410–416.
[52] M. S. Chen, P. Narayanasamy, N. A. Labenz, M. C. White, *J. Am. Chem. Soc.* **2005**, *127*, 6970–6971.
[53] R. I. McDonald, S. S. Stahl, *Angew. Chem. Int. Ed.* **2010**, *49*, 5529–5532.
[54] B. P. Fors, S. L. Buchwald, *J. Am. Chem. Soc.* **2010**, *132*, 15914–15917.
[55] X. Fu, T. Ran, Y. Zhou, J. Liu, *J. Org. Chem.* **2023**, *88*, 6132–6139.
[56] T. J. DeLano, S. E. Reisman, *ACS Catal.* **2019**, *9*, 6751–6754.
[57] Z. Chang, J. Wang, X. Lu, Y. Fu, *Chin. J. Org. Chem.* **2022**, *42*, 147.
[58] W. Chen, S. Ni, Y. Wang, Y. Pan, *Org. Lett.* **2022**, *24*, 3647–3651.
[59] J. J. Habeeb, D. G. Tuck, *J. Chem. Soc. Chem. Commun.* **1976**, 696–697.
[60] T. Shono, I. Nishiguchi, H. Ohmizu, *Chem. Lett.* **1977**, *6*, 1021–1024.
[61] E. Dincan, S. Sibille, J. Perichon, M.-O. Moingeon, J. Chaussard, *Tetrahedron Lett.* **1986**, *27*, 4175–4176.
[62] H. Marzouk, Y. Rollin, J. C. Folest, J. Y. Nédélec, J. Périchon, *J. Organomet. Chem.* **1989**, *369*, C47–C50.
[63] C. Amatore, A. Jutand, J. Périchon, Y. Rollin, *Monatshefte Für Chem. Chem. Mon.* **2000**, *131*, 1293–1304.
[64] M. Onaka, Y. Matsuoka, T. Mukaiyama, *Chem. Lett.* **1981**, *10*, 531–534.
[65] T. Sato, K. Naruse, M. Enokiya, T. Fujisawa, *Chem. Lett.* **1981**, *10*, 1135–1138.
[66] H. Yin, C. Zhao, H. You, K. Lin, H. Gong, *Chem. Commun.* **2012**, *48*, 7034–7036.
[67] A. C. Wotal, D. J. Weix, *Org. Lett.* **2012**, *14*, 1476–1479.
[68] A. H. Cherney, N. T. Kadunce, S. E. Reisman, *J. Am. Chem. Soc.* **2013**, *135*, 7442–7445.
[69] Y. Ai, N. Ye, Q. Wang, K. Yahata, Y. Kishi, *Angew. Chem. Int. Ed.* **2017**, *56*, 10791–10795.
[70] X. Zhou, L. Guo, H. Zhang, R. Y. Xia, C. Yang, W. Xia, *Adv. Synth. Catal.* **2022**, *364*, 1526–1531.
[71] T. Kerackian, D. Bouyssi, G. Pilet, M. Médebielle, N. Monteiro, J. C. Vantourout, A. Amgoune, *ACS Catal.* **2022**, *12*, 12315–12325.
[72] K.-J. Jiao, C. Ma, D. Liu, H. Qiu, B. Cheng, T.-S. Mei, *Org. Chem. Front.* **2021**, *8*, 6603–6608.
[73] B. Zhang, Y. Gao, Y. Hioki, M. S. Oderinde, J. X. Qiao, K. X. Rodriguez, H.-J. Zhang, Y. Kawamata, P. S. Baran, *Nature* **2022**, *606*, 313–318.
[74] R. C. Samanta, J. Struwe, L. Ackermann, *Angew. Chem. Int. Ed.* **2020**, *59*, 14154–14159.
[75] Y. Gao, D. E. Hill, W. Hao, B. J. McNicholas, J. C. Vantourout, R. G. Hadt, S. E. Reisman, D. G. Blackmond, P. S. Baran, *J. Am. Chem. Soc.* **2021**, *143*, 9478–9488.
[76] R. Grigg, B. Putnikovic, C. J. Urch, *Tetrahedron Lett.* **1997**, *38*, 6307–6308.
[77] M. Kuroboshi, *Synlett* **1999**, *1999*, 69–70.
[78] M. Durandetti, J. Périchon, J.-Y. Nédélec, *Tetrahedron Lett.* **1999**, *40*, 9009–9013.
[79] M. Durandetti, J.-Y. Nédélec, J. Périchon, *Org. Lett.* **2001**, *3*, 2073–2076.
[80] K. Namba, Y. Kishi, *Org. Lett.* **2004**, *6*, 5031–5033.
[81] H. Guo, C.-G. Dong, D.-S. Kim, D. Urabe, J. Wang, J. T. Kim, X. Liu, T. Sasaki, Y. Kishi, *J. Am. Chem. Soc.* **2009**, *131*, 15387–15393.
[82] C. Déjardin, A. Renou, J. Maddaluno, M. Durandetti, *J. Org. Chem.* **2021**, *86*, 8882–8890.

[83] M. Durandetti, L. Hardou, R. Lhermet, M. Rouen, J. Maddaluno, *Chem. – Eur. J.* **2011**, *17*, 12773–12783.
[84] S. Xie, Y. Yin, Y. Wang, J. Wang, X. He, R. Bai, R. Shi, *Green Chem.* **2023**, *25*, 1522–1529.
[85] J. L. Oliveira, E. Le Gall, S. Sengmany, E. Léonel, P. Dubot, P. Cénédèse, M. Navarro, *Electrochimica Acta* **2015**, *173*, 465–475.
[86] H. Li, C. P. Breen, H. Seo, T. F. Jamison, Y.-Q. Fang, M. M. Bio, *Org. Lett.* **2018**, *20*, 1338–1341.
[87] R. J. Perkins, A. J. Hughes, D. J. Weix, E. C. Hansen, *Org. Process Res. Dev.* **2019**, *23*, 1746–1751.
[88] M. C. Franke, V. R. Longley, M. Rafiee, S. S. Stahl, E. C. Hansen, D. J. Weix, *ACS Catal.* **2022**, 12617–12626.
[89] D. Mikhaylov, T. Gryaznova, Y. Dudkina, M. Khrizanphorov, S. Latypov, O. Kataeva, D. A. Vicic, O. G. Sinyashin, Y. Budnikova, *Dalton Trans.* **2012**, *41*, 165–172.
[90] X. Hu, I. Cheng-Sánchez, S. Cuesta-Galisteo, C. Nevado, *J. Am. Chem. Soc.* **2023**, *145*, 6270–6279.
[91] C. Zhu, H. Yue, M. Rueping, *Nat. Commun.* **2022**, *13*, 3240.
[92] L. Zhang, X. Hu, *Chem. Sci.* **2020**, *11*, 10786–10791.
[93] Z. Li, W. Sun, X. Wang, L. Li, Y. Zhang, C. Li, *J. Am. Chem. Soc.* **2021**, *143*, 3536–3543.
[94] J. Luo, B. Hu, W. Wu, M. Hu, T. L. Liu, *Angew. Chem. Int. Ed.* **2021**, *60*, 6107–6116.
[95] J. C. Tellis, D. N. Primer, G. A. Molander, *Science* **2014**, *345*, 433–436.
[96] C. Amatore, M. Azzabi, P. Calas, A. Jutand, C. Lefrou, Y. Rollin, *J. Electroanal. Chem. Interfacial Electrochem.* **1990**, *288*, 45–63.
[97] Y. H. Budnikova, J. Perichon, D. G. Yakhvarov, Y. M. Kargin, O. G. Sinyashin, *J. Organomet. Chem.* **2001**, *630*, 185–192.
[98] Z. Zou, H. Li, M. Huang, W. Zhang, S. Zhi, Y. Wang, Y. Pan, *Org. Lett.* **2021**, *23*, 8252–8256.
[99] Y. Ma, J. Hong, X. Yao, C. Liu, L. Zhang, Y. Fu, M. Sun, R. Cheng, Z. Li, J. Ye, *Org. Lett.* **2021**, *23*, 9387–9392.
[100] Z. Zuo, D. T. Ahneman, L. Chu, J. A. Terrett, A. G. Doyle, D. W. C. MacMillan, *Science* **2014**, *345*, 437–440.
[101] Z.-H. Wang, L. Wei, K.-J. Jiao, C. Ma, T.-S. Mei, *Chem. Commun.* **2022**, *58*, 8202–8205.
[102] D. Liu, Z.-R. Liu, Z.-H. Wang, C. Ma, S. Herbert, H. Schirok, T.-S. Mei, *Nat. Commun.* **2022**, *13*, 7318.
[103] P. Zhang, C. "Chip" Le, D. W. C. MacMillan, *J. Am. Chem. Soc.* **2016**, *138*, 8084–8087.
[104] X. Kong, Y. Chen, X. Chen, Z.-X. Lu, W. Wang, S.-F. Ni, Z.-Y. Cao, *Org. Lett.* **2022**, *24*, 2137–2142.
[105] L. Chu, J. M. Lipshultz, D. W. C. MacMillan, *Angew. Chem. Int. Ed.* **2015**, *54*, 7929–7933.
[106] P. Xue, L. Li, N. Fu, *Org. Lett.* **2022**, *24*, 7595–7599.
[107] J. Rein, J. R. Annand, M. K. Wismer, J. Fu, J. C. Siu, A. Klapars, N. A. Strotman, D. Kalyani, D. Lehnherr, S. Lin, *ACS Cent. Sci.* **2021**, *7*, 1347–1355.
[108] "Candidate List of substances of very high concern for Authorisation - ECHA," can be found under https://echa.europa.eu/candidate-list-table, **n.d.**
[109] C. M. Alder, J. D. Hayler, R. K. Henderson, A. M. Redman, L. Shukla, L. E. Shuster, H. F. Sneddon, *Green Chem.* **2016**, *18*, 3879–3890.
[110] M. Klein, S. R. Waldvogel, *Angew. Chem. Int. Ed.* **2022**, *61*, e202204140.
[111] T. Noël, Y. Cao, G. Laudadio, *Acc. Chem. Res.* **2019**, *52*, 2858–2869.
[112] N. Tanbouza, T. Ollevier, K. Lam, *iScience* **2020**, *23*, 101720.

Received: ((will be filled in by the editorial staff))
Accepted: ((will be filled in by the editorial staff))
Published online: ((will be filled in by the editorial staff))